formed with an initial denaturation of 94°C for 30 sec, followed by 30 cycles of heating at 94°C for 30 sec, at 55°C for 2 min, and at 72°C for 1 min. Then 1 μl of the first PCR products were transferred into a second tube containing 49 μl of the reaction buffer as described in the first round reaction, for the second round of the same 30 cycles of amplification, but with the pair of inner primers. The PCR products were detected by electrophoresis on a 1.0% agarose gel in Tris-acetate-EDTA buffer and stained with ethidium bromide (0.4 $\mu g/ml$) and visualized under UV transilluminator, BioDoc-I Imaging System (UVP, Upland, CA, U.S.A.). Positive samples were directly subjected to DNA sequencing for identification of hemoplasma species. The nucleotide sequence of the partial 16S rRNA gene has been deposited in the DDBJ, EMBL, GSDB and NCBI nucleotide sequence databases under the accession number AB550430.

A PCR product was amplified from the five dogs, with expected band size on a 1.0 % agarose gel (Fig. 1). Three are adult dogs suffering from multi-centric lymphoma, starvation, atopic dermatitis, respectively. The other two dogs are puppy (about three months old) and have no sign of disease. No PCR products were amplified from the other 162 dogs, which did not develop any clinical sign of haemolytic anemia due to '*Candidatus* M. haemominutum' infection. Comparison of the obtained sequence (a dog suffered from lymphoma) with those corresponding sequences available in the GenBank database revealed the 98% homology to the 16S rRNA gene of '*Candidatus* M. haemominutum' (Fig. 2). We can not gain sequence of the other 4 PCR products because of insufficient PCR product in the first step PCR.

In this study, we first demonstrated that feline hemoplasma '*Candidatus* M. haemominutum' infected dogs in the northern part of Japan. The relatively low prevalence in dogs in this study, as compared to the feline infection rate of '*Candidatus* M. haemominutum' in Japan [6], may be based on the present study included healthy dog population. The study has certain limitations because of the relatively small number of case analyzed.

These dogs infected with hemoplasma had been kept in the ectoparasite-free conditions and no clinical signs of hemolytic anemia by '*Candidatus* M. haemominutum'. It is known that '*Candidatus* M. haemominutum' infection rarely results in significant clinical signs and anemia is not usually apparent in cat [5]. Similarly, dogs infected with '*Candidatus* M. haemominutum' lacked any clinical signs of hemolytic anemia. The pathogenicity of '*Candidatus* M. haemominutum' may be not severe in the dogs.

The transmission route of '*Candidatus* M. haemominutum' from the cats to the dog is currently unknown. Blood-sucking arthropods (e.g., flees, ticks) have been suspected as natural means of hemoplasma transmission [24]. However, there were not so much tick infestions due to the cold climate in the Tohoku area compared to the southern parts in Japan. It is also possible that the infection was occurred by horizontal transmission from infected cats. There is some

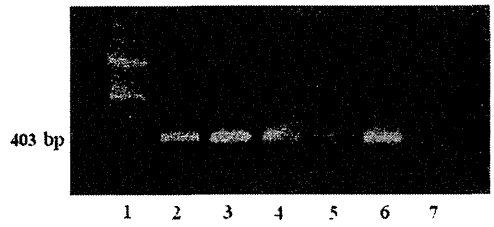

Fig. 1. A representative PCR result on detection for feline '*Candidatus* M. haemominutum' in the dogs. Lane 1 shows 200-bp DNA Ladder (TaKaRa-Bio, Shiga, Japan); Lanes 2–6 show 403-bp DNA fragment. Lanes 2, 3 and 4 dogs suffered from multi-centric lymphoma, starvation, atopic dermatitis, respectively. Lanes 5 and 6; healthy puppy; Lane 7; negative control (water).

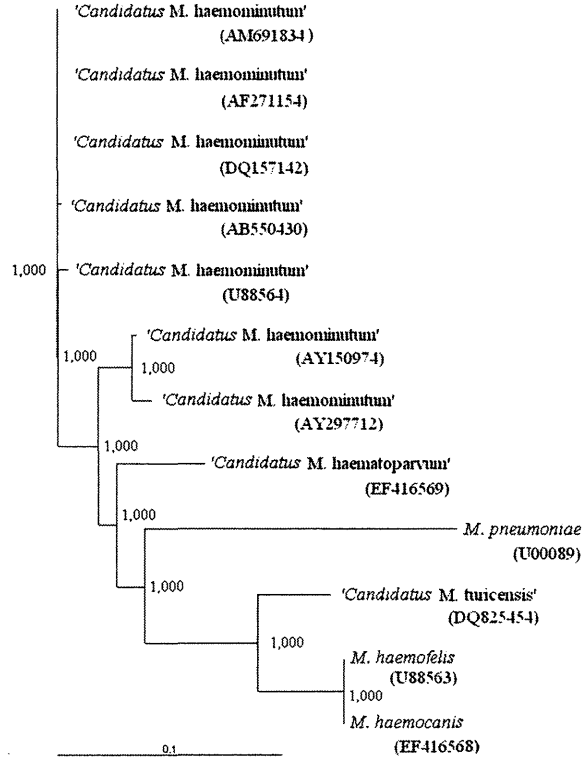

Fig. 2. Phylogenetic tree based on the 16S rRNA sequence comparison among feline and canine hemoplasmas. Genetic distances were computed with CLUSTAL W [14]. Hemoplasma sequences used in this analysis were as follows: '*Candidatus* M. haematoparvum' (EF416569), '*Candidatus* M. haemominutum '(AB550430, AF271154, AM691834, DQ157142, U88564, AY150974, AY297712), '*Candidatus* M. turicensis' (DQ825454), *M. haemocanis* (EF416568), and *M. haemofelis* (U88563). Out-group unit was M. pnemoniae (U00089). Numbers in the relevant branches refer to the values of boot-strap probability of 1,000 replications. Scale bar indicates the evolutionary distance value of 0.1 (a single nucleotide substitution per 10 nucleotides). AB550430 represents a hemoplasma strain detected from a dog (suffered from multi-centric lymphoma) in the present study.

evidence for direct transmission of hemoplasma in cat [24]. In dog, direct transmission of hemoplasmas is one the likely routes. There is also the possibility of transplacental infection [13]. Since we detected '*Candidatus* M. haemominutum' from the two puppies of three months old, there is another likely route of the vertical transmission of '*Candidatus* M. haemominutum' in dogs. The mechanisms of transmission of hemoplasma between dogs and cats have yet to be defined and need further exploration. Zhuang *et al.* [25] suggested the possibility that a dog was one of the hosts for the feline hemoplasma '*Candidatus* M. haemominutum'. However, it is likely that the presence of some underlying conditions (e.g., immunosuppressive, immature) may destroy the strict host specificity in mycoplasma infections, as previously reported in the cases of hemoplasma infection in human [3, 10, 11, 17]. Also, our results may indicate that dogs represent one of the hosts for the feline '*Candidatus* M. haemominutum'.

In conclusion, we first showed feline hemoplasma '*Candidatus* M. haemominutum' infected with dogs in Japan.

ACKNOWLEDGMENT. We thank Dr. Kou Chiba, the director of Will animal hospital, for the useful advice.

REFERENCES

1. Berent, L. M., Messick, J. B. and Cooper, S. K. 1998. Detection of *Haemobartonella felis* in cats with experimentally induced acute and chronic infections, using a polymerase chain reaction assay. *Am. J. Vet. Res.* **59**: 1215–1220.
2. Bobade, P. A., Nash, A. S. and Rogerson, P. 1988. Feline haemobartonellosis: clinical, haematological and pathological studies in natural infections and the relationship to infection with feline leukaemia virus. *Vet. Rec.* **122**: 32–36.
3. Duarte, M. I., Oliveira, M. S., Shikanai-Yasuda, M. A., Mariano, O. N., Takakura, C. F., Pagliari, C. and Corbett, C. E. 1992. Haemobartonella-like microorganism infection in AIDS patients: ultrastructural pathology. *J. Infect. Dis.* **165**: 976–977.
4. Flint, J. C., Roepke, M. H. and Jensen, R. 1959. Feline infections anemia. II. Experimental cases. *Am. J. Vet. Res.* **20**: 33–40.
5. Foley, J. E. and Pedersen, N. C. 2001. '*Candidatus* Mycoplasma haemominutum', a low-virulence epierythrocytic parasite of cats. *Int. J. Syst. Evol. Microbiol.* **51**: 815–817.
6. Fujihara, M., Watanabe, M., Yamada, T. and Harasawa, R. 2007. Occurrence of '*Candidatus* Mycoplasma turicensis' infection in domestic cats in Japan. *J. Vet. Med. Sci.* **69**: 1061–1063.
7. Harvey, J. W. 1998. pp. 166–171. *In*: Infectious Diseases of the Dog and Cat (Greene, C.E. ed.), WB Saunders, Philadelphia.
8. Hoskins, J. D. 1991. Canine haemobartonellosis, canine hepatozoonosis, and feline cytauxzoonosis. *Vet. Clin. North Am. Small Anim. Pract.* **21**: 129–140.
9. Hu, Z., Yin, J., Shen, K., Kang, W. and Chen, Q. 2009. Outbreaks of hemotrophic mycoplasma infections in China. *Emerg. Infect. Dis.* **15**: 1139–1140.
10. Kallick, C. A., Levin, S., Reddi, K. T. and Landau, W. L. 1972. Systemic lupus erythematosus associated with haemobartonella-like organisms. *Nat. New Biol.* **236**: 145–146.
11. Kallick, C. A., Thadhani, K. C. and Rice, T. W. 1980. Identification of Anaplasmataceae (Haemobartonella) antigen and antibodies in systemic lupus erythematosus. *Arthritis Rheum.* **23**: 197–205.
12. Kenny, M. J., Shaw, S. E., Beugnet, F. and Tasker, S. 2004. Demonstration of two distinct hemotropic mycoplasmas in French dogs. *J. Clin. Microbiol.* **42**: 5397–5399.
13. Krakowka, S. 1977. Transplacentally acquired microbial and parasitic diseases of dogs. *J. Am. Vet. Med. Assoc.* **171**: 750–753.
14. Lester, S. J., Hume, J. B. and Phipps, B. 1995. *Haemobartonella canis* infection following splenectomy and transfusion. *Can. Vet. J.* **36**: 444–445.
15. Messick, J. B. 2003. New perspectives about hemotrophic mycoplasma (formerly, *Haemobartonella* and *Eperythrozoon* species) infections in dogs and cats. *Vet. Clin. North Am. Small Anim. Pract.* **33**: 1453–1465.
16. Messick, J. B. 2004. Hemotrophic mycoplasmas (hemoplasmas): a review and new insights into pathogenic potential. *Vet. Clin. Pathol.* **33**: 2–13.
17. Santos, A. P., Santos, R. P., Biondo, A. W., Dora, J. M., Goldani, L. Z., de, Oliveira, S. T., de, Sa, Guimaraes, A. M., Timenetsky, J., de, Morais, H. A., Gonzalez, F. H. and Messick, J. B. 2008. Hemoplasma infection in HIV-positive patient, Brazil. *Emerg. Infect. Dis.* **14**: 1922–1924.
18. Sykes, J. E., Bailiff, N. L., Ball, L. M., Foreman, O., George, J. W. and Fry, M. M. 2004. Identification of a novel hemotropic mycoplasma in a splenectomized dog with hemic neoplasia. *J. Am. Vet. Med. Assoc.* **224**: 1946–1951, 1930–1931.
19. Sykes, J. E., Drazenovich, N. L., Ball, L. M. and Leutenegger, C. M. 2007. Use of conventional and real-time polymerase chain reaction to determine the epidemiology of hemoplasma infections in anemic and nonanemic cats. *J. Vet. Intern. Med.* **21**: 685–693.
20. Thompson, J. D., Higgins, D. G. and Gibson, T. J. 1994. CLUSTAL W: improving the sensitivity of progressive multiple sequence alignment through sequence weighting, position-specific gap penalties and weight matrix choice. *Nucleic Acids Res.* **22**: 4673–4680.
21. Watanabe, M., Hisasue, M., Souma, T., Ohshiro, S., Yamada, T. and Tsuchiya, R. 2008. Molecular detection of *Mycoplasma haemofelis* and '*Candidatus* Mycoplasma haemominutum' Infection in cats by direct PCR using whole blood without DNA extraction. *J. Vet. Med. Sci.* **70**: 1095–1099.
22. Wengi, N., Willi, B., Boretti, F. S., Cattori, V., Riond, B., Meli, M. L., Reusch, C. E., Lutz, H. and Hofmann-Lehmann, R. 2008. Real-time PCR-based prevalence study, infection follow-up and molecular characterization of canine hemotropic mycoplasmas. *Vet. Microbiol.* **126**: 132–141.
23. Westfall, D. S., Jensen, W. A., Reagan, W. J., Radecki, S. V. and Lappin, M. R. 2001. Inoculation of two genotypes of *Hemobartonella felis* (California and Ohio variants) to induce infection in cats and the response to treatment with azithromycin. *Am. J. Vet. Res.* **62**: 687–691.
24. Willi, B., Boretti, F. S., Tasker, S., Meli, M. L., Wengi, N., Reusch, C. E., Lutz, H. and Hofmann-Lehmann, R. 2007. From *Haemobartonella* to hemoplasma: molecular methods provide new insights. *Vet. Microbiol.* **125**: 197–209.
25. Zhuang, Q. J., Zhang, H. J., Lin, R. Q., Sun, M. F., Liang, X. J., Qin, X. W., Pu, W. J. and Zhu, X. Q. 2009. The occurrence of the feline "*Candidatus* Mycoplasma haemominutum" in dog in China confirmed by sequence-based analysis of ribosomal DNA. *Trop. Anim. Health Prod.* **41**: 689–692.

Journal of Virological Methods 174 (2011) 166–172

Contents lists available at ScienceDirect

Journal of Virological Methods

journal homepage: www.elsevier.com/locate/jviromet

Short communication

Species characterization in the genus *Pestivirus* according to palindromic nucleotide substitutions in the 5′-untranslated region

Massimo Giangaspero*, Ryô Harasawa

Veterinary Microbiology, School of Veterinary Medicine, Faculty of Agriculture, Iwate University, 18-8, Ueda 3 Chome, Morioka 020-8550, Iwate, Japan

Article history:
Received 23 April 2010
Received in revised form 25 March 2011
Accepted 5 April 2011
Available online 12 April 2011

Keywords:
Palindromic nucleotide substitutions
Pestivirus
Taxonomy
5′-UTR

A B S T R A C T

The palindromic nucleotide substitutions (PNS) at the three variable loci (V1, V2 and V3) in the 5′-untranslated region (UTR) of the *Pestivirus* genome have been considered for taxonomical segregation of the species, through the evaluation of 534 strains. On the basis of qualitative and quantitative secondary structure characteristics, species have been identified within the genus, determining genetic distances between species isolates, clarifying borderline and multirelated sequences, and characterizing and clustering the *Pestivirus* strains showing unexpected genomic sequences. Nine genomic groups have been identified: the species *Bovine viral diarrhea virus 1* (BVDV-1), *Bovine viral diarrhea virus 2* (BVDV-2), *Border disease virus* (BDV) and *Classical swine fever virus* (CSFV) and the tentative species Pronghorn, Giraffe, *Bovine viral diarrhea virus 3* (BVDV-3) (HoBi group), *Border disease virus 2* (BDV-2) (Italian small ruminant isolates) and Bungowannah.

Palindromic positions have been characterized according to changes in nucleotide base-pairs identifying low variable positions (LVP) including base-pairs present in less than 80% of the genus. The determination of divergence between single strain sequences or genetic groups was obtained easily by comparing base-pairing combinations from aligned secondary structures. This provided clear information such as the level of heterogeneity within a species, the relatedness between species, or facilitating the characterization and clustering of specific strains. The BVDV-1 and BDV species resulted heterogeneous, showing isolates located on a borderline in the species. Within the BVDV-2 species, two main genogroups were identified, with strains showing common sequence characteristics to both groups (multirelated strains). They could be allocated correctly by quantitative analysis. Similarly, the relation between CSFV and BDV species appeared very clearly. Also in this case, ambiguous strain sequences could be clustered in the species showing the lowest divergence values.

In conclusion, the proposed taxonomical procedure is based on the evaluation of only the strategic and highly conserved genome regions in the 5′-UTR. Furthermore, the application of quantitative analytical procedure allowed for a better determination of relation among species.

The genus *Pestivirus* of the family *Flaviviridae* is represented by four established species *Bovine viral diarrhea virus 1* (BVDV-1), *Bovine viral diarrhea virus 2* (BVDV-2), *Border disease virus* (BDV) and *Classical swine fever virus* (CSFV) and a tentative "Giraffe" species (Fauquet et al., 2005). These viruses infect a wide range of ungulate species like swine, cattle and sheep. They can cause prenatal and postnatal infections and heavy economical losses. Persistently infected animals are the main source of infection.

The pestiviruses were classified generally into different viral species according to their host origin: CSFV in pig, BVDV-1 and BVDV-2 in cattle, and BDV in sheep. However, cross infection may occur, thus, this approach resulted not sustainable. Therefore, isolates have to be classified according to their genetic sequence characteristics and the relatedness to viral strains that are used to define the type species. The Pestiviruses genome has a single-stranded, positive polarity RNA, composed by a sequence of about 12,500 nucleotides. It can be divided into three regions: a 5′-untranslated region (UTR), a single large open reading frame encoding a polyprotein, and a 3′-UTR. The virus-encoded polyprotein is cleaved into structural (C, Erns, E1 and E2) and non-structural proteins (Npro, P7, NS2-3, NS4A, NS4B, NS5A, NS5B). Previous reported phylogenetic analysis used different genomic regions, namely 5′-UTR, Npro or E2 genes, to distinguish genotypes within

* Corresponding author at: School of Veterinary Medicine, Faculty of Agriculture, Iwate University, 18-8, Ueda 3 Chome, Morioka 020-8550, Iwate, Japan.
Tel.: +81 196216158.
E-mail addresses: giangasp@iwate-u.ac.jp, giangasp@gmail.com (M. Giangaspero).

0166-0934/$ – see front matter © 2011 Elsevier B.V. All rights reserved.
doi:10.1016/j.jviromet.2011.04.004

Table 1
Summary of *Pestivirus* strains (*n* 534) evaluated according to the palindromic nucleotide substitution (PNS) method at the 5′-untranslated region of RNA.

Species	Number of strains	Host	Geographical origin
BVDV-1	274	Cattle, sheep, pig, deer, roe deer, human, contaminant	Argentina, Austria, Belgium, Brazil, Canada, China, Belgium, France, Germany, India, Ireland, Italy, Japan, New Zealand, Slovakia, South Africa, Spain, Sweden, Switzerland, UK, USA
BVDV-2	77	Cattle, sheep, contaminant	Argentina, Austria, Belgium, Brazil, Canada, France, Germany, Italy, Japan, Netherland, NewZealand, Slovakia, Tunisia, UK, USA
BVDV-3[a]	3	Cattle	Brazil, Thailand
BDV	131	Sheep, pyrenean chamois, cattle, pig, reindeer, wisent	Australia, France, Germany, Japan, New Zealand, Spain, Switzerland, Tunisia, Turkey, UK, USA
BDV-2[a]	3	Sheep, goat	Italy
CSFV	43	Pig, sheep	China, France, Garmany, Honduras, Italy, Japan, Malaysia, Netherlands, Poland, Russia, Spain, Switzerland, USA
Pronghorn[a]	1	Pronghorn	USA
Giraffe[a]	1	Giraffe	Kenya
Bungowannah[a]	1	Pig	Australia

[a] Tentative species.

each viral species. Npro refers to an N-terminal autoprotease that has no counterpart in other flaviviruses, whereas the E2 protein plays a major role in virus attachment and entry. In addition, E2 is also important for the induction of neutralizing antibodies. So far, genotyping using 5′-UTR, Npro or E2 sequences has given consistent results. As the 5′-UTR is relatively more conserved among all members within the genus, this genomic region was used to define pan-pestivirus reactive primers (Vilček et al., 1994), and was also more frequently utilised for the characterization of genotypes. Primary structure analysis, by sequence alignment and construction of phylogenetic trees, is the most common method for the classification of the virus isolates.

The nucleotide substitutions occurring at the level of the 5′-UTR genomic region are particularly important, since positive-sense RNA viruses include generally regulatory motifs, which are indispensable for viral survival. In Pestiviruses, the secondary structure of the 5′-UTR includes an internal ribosomal entry site (IRES), responsible for translational, transcriptional and replicational events (Deng and Brock, 1993). Thus, stable nucleotide variations at this level assume great importance in terms of virus evolutionary history. Nucleotide sequences at the variable loci, V1, V2 and V3, in the 5′-UTR of pestiviruses have been shown to be capable of forming a stable stem–loop structure peculiar to each *Pestivirus* species. The observation of nucleotide variations among virus strains at the level of the three specific variable loci in the secondary structure of the 5′-UTR has been conceived as a simple and practical procedure for genotyping (Harasawa and Giangaspero, 1998). The palindromic nucleotide substitutions (PNS) genotyping method has been further improved from the original concept limited to qualitative analysis (Giangaspero and Harasawa, 2007), allowing the taxonomical segregation of the genus *Pestivirus* into six species: BVDV-1, BVDV-2, CSFV, BDV, the tentative species Giraffe and a new proposed taxon named Pronghorn.

The relatively large number of new deposited sequences of isolates from domestic and wild animals and the recent evidence of novel "atypical" *Pestivirus* sequences, as for example the strains D32/00_'HoBi' (Schirrmeier et al., 2004) and Th/04_KhonKaen (Liu et al., 2009a) isolated in cattle infected naturally, in Brazil and Thailand, respectively, or the Bungowannah virus isolated from piglets in Australia (Kirkland et al., 2007), motivated the necessity for a updated application of the PNS method.

Qualitative and quantitative evaluation of genomic sequence divergence, in terms of palindromic nucleotide base pairings variations, has been applied for taxonomical segregation of species, through the evaluation of 534 genomic sequences. The nucleotide sequences in the 5′-UTR of *Pestivirus* strains, with different geographical origins, from different host species or contaminants of biological products, were obtained from the GenBank DNA database, provided by authors or obtained in our laboratories (Table 1) (detailed list of analysed strains available under request).

Nucleotide sequence secondary structures were predicted according to the algorithm of Zuker and Stiegler (1981) using the Genetyx-Mac version 10.1 program package (Software Development Co., Ltd., Tokyo, Japan). The minimum free energy was calculated by the method of Freier et al. (1986). Relevant secondary structure regions in the 5′-UTR were used for genotyping based on the palindromic nucleotide substitutions method (Harasawa and Giangaspero, 1998; Giangaspero and Harasawa, 2007). The identification of species within the genus has been achieved according to highly conserved base pairs in the three variable palindromic loci, based on a series of specific passages focused on the qualitative and quantitative analysis of the secondary structures of the strains in the genus. The first step was qualitative and consisted in the characterization of the different positions of the 3 stems and loops in the 5′-UTR sequences of all the considered strains belonging to the genus. Variable loci were positioned in the prototype *Pestivirus* strain BVDV-1 Osloss sequence (De Moerlooze et al., 1993) as follows: V1 197-235, V2 267-289 and V3 293-311. Only V2 locus was composed by a constant number of nucleotides (*n* 23). The variation of loops in V1 and V3 loci determined difference in size of palindromes. Secondary structure sequences showing divergent base pair combinations have been aligned for comparison. For strain comparison, differences in number and type of nucleotides constituting the palindromes have been considered (Giangaspero and Harasawa, 2007). Palindromic positions have been characterized according to changes in nucleotide base pairs identifying low variable positions (LVP) including base pairs present in less than 80% in the genus, thus, selecting specific base pairings suitable for genus and species determination. The second step was quantitative, allowing the identification of genomic groups among *Pestivirus* strains by clustering the base pair combinations according to LVP. Cross comparisons between types within the genus have been evaluated by computing the divergence percentage, identifying strains showing multirelation or borderlines, and quantifying the heterogeneity of a species and the genetic distance between species in terms of variation of base pairs in the secondary structure (Table 3).

The observation made on the nucleotide sequences of the three variable loci at the level of the 5′-UTR genomic region of *Pes-*

Table 2
Palindromic nucleotide substitutions (PNS) characteristic to the genus *Pestivirus*. The position of base pairings is defined by numbering from the bottom of the variable locus.

	Locus	Characteristic PNS markers
Genus		
	V1	Absence in position 22—size of V1 21 bp (exception U); C C bulge in position 11; A-U in position 10; C-G in position 8 (exceptions U*G, U-A and G G bulge); U-A in position 7 (exception G-C and A A bulge); A in position 6 (exception G); U*G in position 5; U in position 5 right nucleotide; G-C in position 4.
	V2	GGGGU loop (exception GGGGC); C-G in position 8 (exception U*G).
Species		
BVDV-1	V1	U-A in position 15 (exception U*G or C-G);
	V2	G-C in position 5 (exception A-U);
	V3	G-C in position 5; A in position 10 (exceptions R:H).
BVDV-2	V1	A-U or A C bulge in position 20 (exceptions Z:H); A,G or U in position 21 (exception GG);
	V2	U-A or U*G in position 6 (exception C A bulge);
	V3	A-U or A C bulge in position 7 (exception G-C).
BVDV-3 tentative species (HoBi group)	V1	U-A in position 15;
	V3	G-C or G*U in position 3; A-U or G-C in position 7; A in position 10.
BDV	V1	G-C or A-U in position 15 (exceptions C U and A C bulges);
	V3	U C and U U bulges or U*G in position 7 (exceptions A-U, U-A and C C, A C, C U and C A bulges).
BDV-2 tentative species (Italian ovine isolates)	V1	U-A or C A bulge in position 15;
	V3	G*U or G G bulge in position 8.
CSFV	V1	U-A in position 13 (exception U*G);
	V3	U-A in position 2; U or C in position 8 (exception A).
Pronghorn tentative species	V1	G-C in position 2; U-A in position 9; U-A in position 12; U-A in position 15;
	V2	G-C in position 4;
	V3	G A bulge in position 5.
Giraffe tentative species	V1	C-G in position 2; U*G in position 20;
	V2	C-G in position 7;
	V3	C-G in position 4; G*U in position 7.
Bungowannah tentative species	V1	A-U in position 2; G-C in position 7; U-A in position 9; U-A in position 12; G-C in position 13;
	V2	A-U in position 3; G-C in position 4;
	V3	U-A in position 4; G A bulge in position 10; A in position 11.

Table 3
Identified species within genus *Pestivirus*.

(A) Relations within species

Species	Divergence within genus	Divergence within species %/mean value	Multirelated strains	Borderline strains
BVDV-1	0.33	6.43/9.54	None	3186V6, J, R, S, MV98CB95, W, ZM-95
BVDV-2	2.00	11.15/7.89	None	None
BVDV-2A	1.93	0.40/5.37	vs 2B 713-2, 5521-95, BSE1239, UVR420, 97/730	
BVDV-2B	2.25	0/7.28	vs 2A VS-123.4, VS-63	
BVDV-3	2.00	0/4	None	None
BDV	2.22	27.89/11.22	vs CSFV 91-F-6731, 91-F-6732	Aydin/04-TR, Burdur/05-TR
BDV-2	2.33	0/4.5	None	None
CSFV	2.33	0/5.52	vs BDV Kanagawa/74	None
Pronghorn	4	0/0	None	None
Giraffe	7	0/0	None	None
Bungowannah	7	0/0	None	None

(B) Relations among species

Species	Divergence %/divergence value mean									
BVDV-2	100/19.53									
BVDV-2A	100/19.78									
BVDV-2B	100/18.54		33.20/12.85							
BVDV-3	100/16.94	100/17.10	100/17.02	100/17.41						
BDV	100/19.70	100/18.73	100/18.57	100/19.38	100/18.83					
BDV-2	99.62/17.86	100/17.79	100/17.71	100/18.08	100/19.33	97.74/16.30				
CSFV	100/19.29	100/20.68	100/20.63	100/20.88	100/19.51	69.30/14.48	100/17.13			
Pronghorn	100/19.43	100/21.02	100/20.64	100/22.50	100/19.00	100/20.39	100/17.00	100/21.83		
Giraffe	100/26.00	100/20.17	100/19.84	100/21.50	100/23.33	100/21.66	100/20.33	100/23.38	100/22.00	
Bungowannah	100/24.23	100/26.07	100/26.15	100/25.75	100/25.00	100/25.98	100/24.66	100/24.05	100/22.00	100/30.00
	BVDV-1	BVDV-2	BVDV-2A	BVDV-2B	BVDV-3	BDV	BDV-2	CSFV	Pronghorn	Giraffe

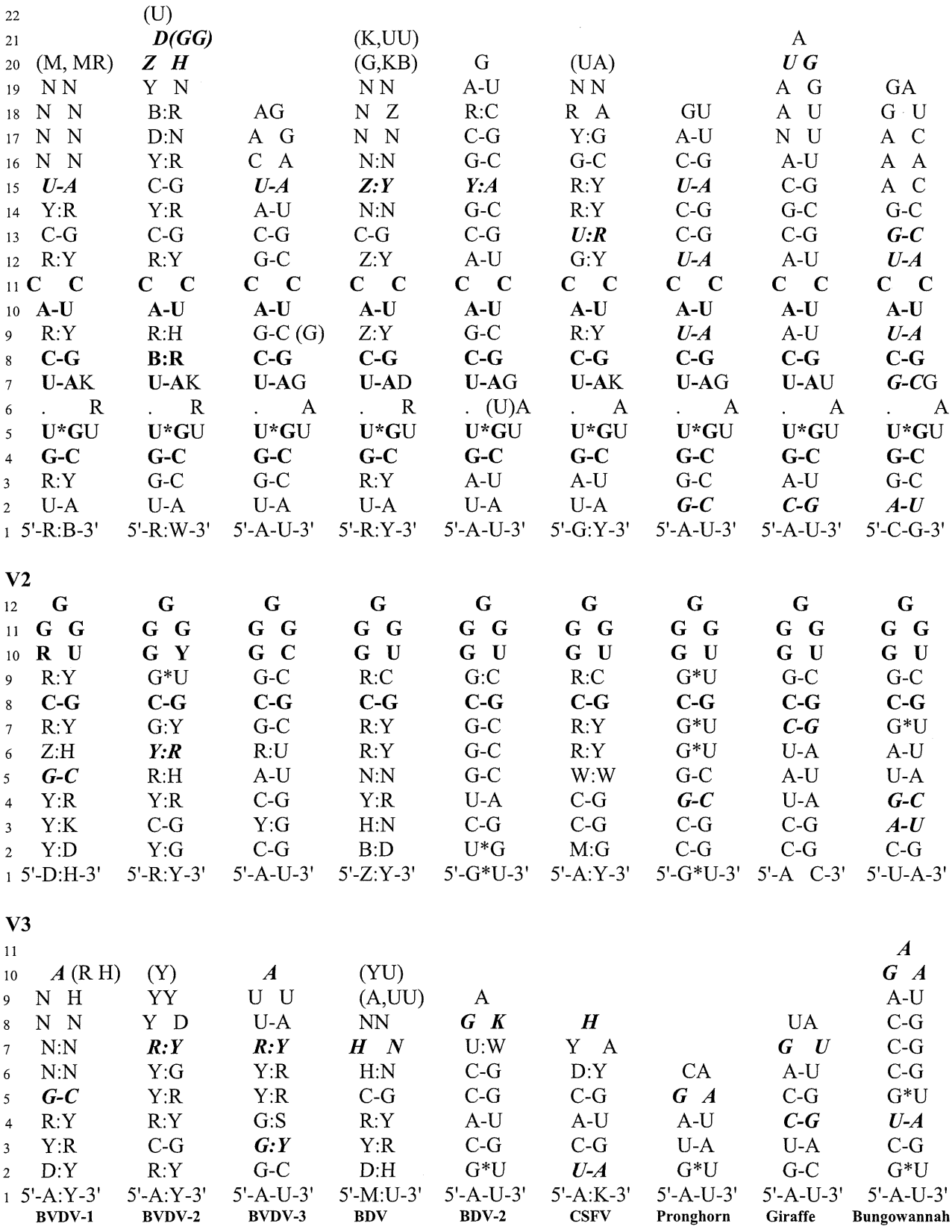

Fig. 1. V1–V3 palindromic loci in the 5′-UTR of the genus *Pestivirus* species. Base pairings characteristic to the genus (PNS genus specific) are shown in bold. The characteristic base pairings of the species BVDV-1, BVDV 2, BDV, CSFV, and the new proposed taxons BVDV-3, BDV-2, Giraffe, Pronghorn and Bungowannah (PNS species specific) are represented in bold and italic. The position of base-pairings is defined by numbering from the bottom of the secondary structures. Watson–Crick base pairings are indicated by a dash (-); tolerated pairings in secondary structure are indicated by an asterisk (*); interchangeable base pairings are indicated by a column (:). M = A or C; R = A or G; W = A or U; S = C or G; Y = C or U; K = G or U; Z = A or C or G; H = A or C or U; D = A or G or U; B = C or G or U; N = A or C or G or U.

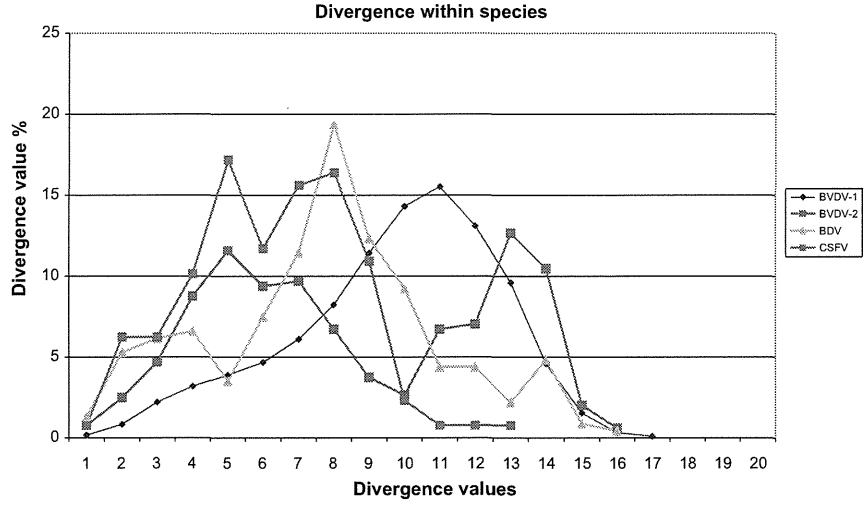

Fig. 2. Determination of the level of heterogeneity within the single species in the genus *Pestivirus* (PNS method). The divergence values between single strain sequences were obtained by comparing base pairing from aligned secondary structure sequences, helping for the characterization and clustering of specific strains. Species divergence limit value was 13. Within the BVDV-2 species, heterogeneity was particularly marked, represented graphically by a curve characterized by two distinct peaks. The left peak (low divergence values) was related to homogeneity within groups. Comparison of homogeneous groups resulted in higher divergence values (right peak), indicating clear divergence between the groups. This corresponded to two identifiable main genogroups: BVDV-2A, characterized by a cosmopolitan diffusion, and BVDV-2B, restricted to South America. In both groups, some strains showed common sequence characteristics to both groups (multirelated strains). They could be allocated correctly by quantitative analysis.

tivirus strains, according to the PNS genotyping method, allowed to the identification of consensus motifs shared by all the *Pestivirus* species, genus specific base-pairings positioned in the V1 and V2 loci, and characteristic species specific PNS, respectively (Table 2). On the base of qualitative and quantitative secondary structure characteristics, nine species have been identified: *Bovine viral diarrhea virus 1* (BVDV-1), *Bovine viral diarrhea virus 2* (BVDV-2), *Classical swine fever virus* (CSFV), *Border disease virus* (BDV), and the tentative species Pronghorn, Giraffe, *Bovine viral diarrhea virus 3* (BVDV-3) (HoBi group), *Border disease virus 2* (BDV-2) (Italian small ruminant isolates) and Bungowannah. The secondary structure variable loci in the 5′-UTR of the *Pestivirus* species are reported in Fig. 1. The genetic markers useful for taxonomic purposes identified at genus level were represented by base pairings from highly conserved, homogeneous positions. At species level, characteristic base pairings determinative for species identification (species determinative at genus level (SDG) not shared with other species) were identified from conserved positions only in BVDV-3, Pronghorn, Giraffe and Bungowannah species. However, clear identification for BVDV-1, BVDV-2, BDV, BDV-2 and CSFV species was obtained using specific combinations of base-pairings in the sequence (species determinative (SD) from conserved positions species specific, shared with other species). These base-pairings acquired significance only when combined, and they were non specific when considered separately.

The palindromic structures were identifiable in linear sequences. However, it was easier to find them observing the secondary structure. The evaluation of the secondary structure based on a qualitative observation of the nucleotide variations was supported and confirmed through the application of a quantitative approach. The determination of divergence between single strain sequences or genetic groups was obtained easily by comparing base pairing from aligned secondary structure sequences. This provided clear information such as the level of heterogeneity within a species, the genetic distance between species in terms of variation of base pairs in the secondary structure, or helping for the characterization and clustering of specific strains (Table 3). The BVDV-1 and BDV species resulted heterogeneous, showing borderline strain sequences. Strains 3186V6, J, R, S, W (Vilček et al., 2001), and MV98CB95 (Baule et al., 1997) isolated from cattle, and the pig strain ZM-95 (Xu et al., 2006) were located on a borderline in the BVDV-1 species. Their sequences showed qualitative similarities with the BVDV-1 species, sharing partially the specific PNS species markers, but with high divergence values, thus, candidates for reclustering as separate groups in the genus. Similarly, the strains Aydin/04-TR and Burdur/05-TR (Oguzoglu et al., 2009), isolated from sheep in Turkey, showing partial genetic relatedness only with members of the BDV species, were clustered in the species as borderline. Within the BVDV-2 species, heterogeneity was particularly marked, represented graphically by a curve characterized by two distinct peaks (Fig. 2). The left peak (low divergence values) was related to homogeneity within groups. Comparison of homogeneous groups resulted in higher divergence values (right peak), indicating clear divergence between the groups. However, mean divergence value (12.85) did not allowed their segregation into different species. This corresponded to two identifiable main genogroups: BVDV-2A, characterized by a cosmopolitan diffusion, and BVDV-2B, restricted to South America. In both groups, some strains showed common sequence characteristics to both groups (multirelated strains). They could be allocated correctly by quantitative analysis. Similarly, the relation between CSFV and BDV species appeared very clearly (Fig. 3), as example of the genetic relatedness determination among *Pestivirus* species. The computing of the divergence by comparing sequences from both species showed very low values (mean 14.48) when compared to those obtained with other *Pestivirus* species (from 17 and 17.13 with Pronghorn and BDV-2, to 24.05 with Bungowannah) (Table 3). Also in this case, ambiguous strains, sharing common sequence characteristics to both species (multirelated strains), could be clustered in the species showing the lowest divergence values.

The classification among *Pestivirus* species strains according to PNS analysis based on changes in the secondary structure was compared with those based on the 5′-UTR primary structure, carried out through alignment and construction of phylogenetic trees. The results were generally comparable. In particular, new taxons have been defined due to specific base-pairings, despite the limited number of allocated strains. This corresponded to the observations made by different investigators, evaluating the 5′-UTR or other genomic regions (Schirrmeier et al., 2004; Vilček et al., 2005; Cortez et al., 2006; Kirkland et al., 2007). However, some atypical strains were

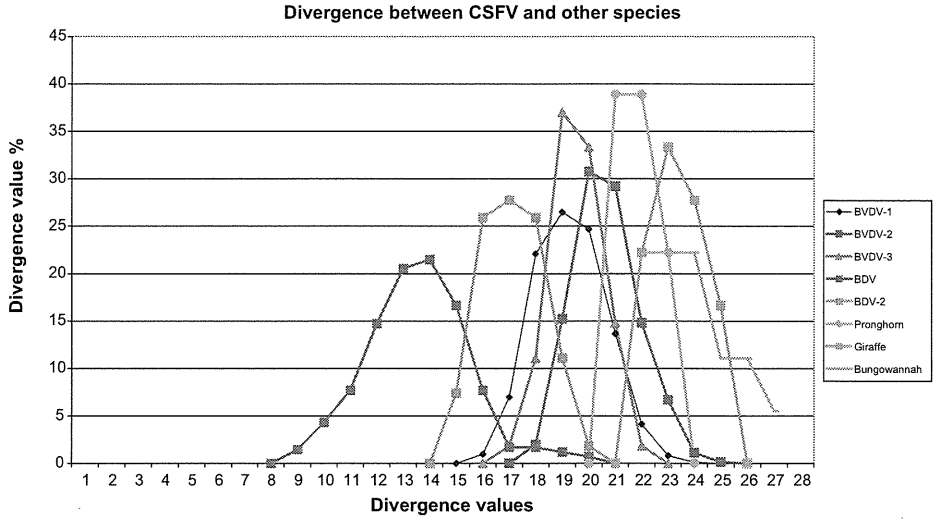

Fig. 3. Determination of the genetic relatedness among *Pestivirus* species (PNS method). The comparison of CSFV strain 5′-UTR sequences with those from other species showed a very clear relation between CSFV and BDV species, with very low divergence values (mean 14.48). Ambiguous strains, sharing common sequence characteristics to both species (multirelated strains), could be clustered in the species showing the lowest divergence values.

related to controversial taxonomical clustering, in particular for sequences isolated from small ruminants. The sheep isolates from Tunisia (strains 33S, 35, 35T, Lot21, SN1T, SN3G, SN2T, 37A, RM and BM01 isolate 5), reported by Thabti et al. (2005), associated to clinical cases due to the use of a vaccine produced on contaminated cell lines derived from ovine, and natural infections, represented an interesting pestivirus intermediate group, genetically close to CSFV but antigenically related to BDV. They have been reported by the author as members of a new genotype of the BDV species. Two French ovine isolates, 91-F-6731 and 91-F-6732 (Dubois et al., 2008), showed high genetic similarity with the Tunisian strains. The author indicated that both group of strains belong to a novel species named Tunisian. Other studies reported the Tunisian strains as a separate species (Valdazo-Gonzalez et al., 2006, 2007; Liu et al., 2009b), or belonging to the BDV species (De Mia et al., 2005). The application of PNS segregated these isolates in the BDV species, based on the divergence values when compared to CSFV and BDV sequences, despite the sharing of CSFV specific base pairing U-A in position 2 in V3. In particular, the Tunisian and French isolates constituted a homogeneous group with divergence mean of 5.5 within the group. The strains showed lower divergence values with BDV than with CSFV, mean 12.07 and 12.72, respectively. Furthermore, the strains 712/02 (De Mia et al., 2005), LA/91/05 (Giammarioli et al., unpublished) and TO/121/04 (De Mia, unpublished) isolated from small ruminants in Italy, and reported as genotype of BDV species, have been clustered as new taxon in the genus *Pestivirus*, showing a divergence value mean of 16.30 with the BDV species. The ovine strains 098, 119 and 63 from Tunisia (Thabti et al., unpublished) have been clustered within the BVDV-2 species, group BVDV-2A, constituting a separate genotype in addition to the four genotypes, BVDV-2a, BVDV-2b, BVDV-2c, and BVDV-2d previously described (Giangaspero et al., 2008a). In the present study, the nomenclature of HoBi group isolates as BVDV-3, proposed by Liu et al. (2009b), was adopted in reason to the close relation with the BVDV-1 species.

Problematic sequences showing difficulties for clustering based on primary structure analysis highlight the interest of applying PNS in order to clarify possible taxonomical discrepancies. However, as disadvantage, apart the lack of current informatics design of the method, only 5′-UTR is targeted and it is not applicable a combined study approach on different portions of the genome such as Npro, since no other genomic regions have been explored for the application of PNS.

The PNS demonstrated to offer a reliable alternative for viral investigations to classical taxonomical methods based on primary sequence structure. As secondary structures are essential for survival of the viral population, variations in the involved genomic regions might be related with biological characteristics, which in turn might correlate with classification. The relevant role of the 5′-UTR in the translational, transcriptional and replicational mechanisms in pestiviruses implies that its secondary structures (e.g. palindromic structures) must be highly conserved, and that observed mutations are particularly meaningful. Since these mutations are observed as conserved nucleotide changes, they may be considered as the occurrence of a micro evolution step through selection in the phylogenetic history of the virus. On the base of the above mentioned considerations the nucleotide substitutions at the level of the palindromic structures in the genomic 5′-UTR may represent a useful genetic marker for taxonomical procedures in pestiviruses and theoretically for other RNA positive strand viruses. Secondary structures predicted at the variable regions in the 5′-UTR showed typical PNS which were useful for classification or genotyping of hepatitis C virus (Giangaspero et al., 2008b).

In conclusion, the proposed method provides results comparable with other taxonomical procedures based on 5′-UTR primary structure evaluation, but it differs from them in that only the strategic and highly conserved genome regions in the 5′-UTR, and therefore the most meaningful nucleotide sequences at this level, are considered. Thus accurate parameters for species identification in terms of nucleotide sequence homology are made available with great advantage for simplification of virological investigations. Furthermore, the application of quantitative analytical procedure allowed to a better determination of relation among species and genotypes. *Pestivirus* strains showing unexpected genomic sequences such as Giraffe (Plowright, 1969), Wisent Casimir (Becher et al., 1999), Chamois-1 (Arnal et al., 2004), Pronghorn (Vilček et al., 2005), HoBi group strains (Schirrmeier et al., 2004; Cortez et al., 2006; Liu et al., 2009a) and Bungowannah (Kirkland et al., 2007) have been characterized easily and clustered within the genus by PNS method. The procedures require constant adaptability to eventual new and different observations. In addition, further investigations will possibly provide new variants in the species and other genotypes or subtypes might be characterized, requiring subsequent revision of identification markers. Nevertheless, the manual searching of relevant base-pairings and direct observation of the sequences still remain the method's main

limitations. Further efforts are required in order to develop the PNS method in a fully computerized procedure for easy user-access and rapid testing with reliable results.

References

Arnal, M., Fernandez-de-Luco, D., Riba, L., Maley, M., Gilray, J., Willoughby, K., Vilček, S., Nettleton, P., 2004. A novel pestivirus associated with deaths in Pyrenean chamois (*Rupicapra pyrenaica pyrenaica*). J. Gen. Virol. 85, 3653–3657.

Baule, C., van Vuuren, M., Lowings, J.P., Belak, S., 1997. Genetic heterogeneity of bovine viral diarrhoea viruses isolated in Southern Africa. Virus Res. 52 (2), 205–220.

Becher, P., Orlich, M., Kosmidou, M., Baroth, M., Thiel, J.-H., 1999. Genetic diversity of pestiviruses: identification of novel groups and implications for classification. Virology 262, 64–71.

Cortez, A., Heinemann, M.B., de Castro, A.M.M.G., Soares, R.M., Pinto, A.M.V., Alfieri, A.A., Flores, E.F., Leite, R.C., Richtzenhain, L.J., 2006. Genetic characterization of Brazilian bovine viral diarrhea virus isolates by partial nucleotide sequencing of the 5′-UTR region. Pesqui. Vet. Bras. 26 (4), 211–216.

De Mia, G.M., Greiser-Wilke, I., Feliziani, F., Giammarioli, M., De Giuseppe, A., 2005. Genetic characterization of a caprine pestivirus as the first member of a putative novel pestivirus subgroup. J. Vet. Med. B Infect. Dis. Vet. Public Health 52 (5), 206–210.

De Moerlooze, L., Lecomte, C., Brown-Shimmer, S., Schmetz, D., Guiot, C., Vandenbergh, D., Allaer, D., Rossius, M., Chappuis, G., Dina, D., Renard, A., Martial, J.A., 1993. Nucleotide sequence of the bovine viral diarrhoea virus Osloss strain: comparison with related viruses and identification of specific DNA probes in the 5′ untranslated region. J. Gen. Virol. 74, 1433–1438.

Deng, R., Brock, K.V., 1993. 5′ and 3′ untranslated regions of pestivirus genome: primary and secondary structure analyses. Nucleic Acids Res. 21, 1949–1957.

Dubois, E., Russo, P., Prigent, M., Thiéry, R., 2008. Genetic characterization of ovine pestiviruses isolated in France, between 1985 and 2006. Vet. Microbiol. 130, 69–79.

Fauquet, C.M., Mayo, M.A., Maniiloff, J., Desselberger, U., Ball, L.A., 2005. Virus Taxonomy. Classification and Nomenclature of Viruses. Elsevier, Academic Press, San Diego.

Freier, S.M., Kierzek, R., Jaeger, J.A., et al., 1986. Improved free-energy parameters for predictions of RNA duplex stability. Proc. Natl. Acad. Sci. U.S.A. 83, 9373–9377.

Giangaspero, M., Harasawa, R., 2007. Numerical taxonomy of genus *Pestivirus* based on palindromic nucleotide substitutions in the 5′ untranslated region. J. Virol. Methods 146, 375–388.

Giangaspero, M., Harasawa, R., Weber, E.L., Belloli, A., 2008a. Genoepidemiological evaluation of Bovine viral diarrhea virus 2 species based on secondary structures in the 5′ genomic untranslated region. J. Vet. Med. Sci. 70 (6), 571–580.

Giangaspero, M., Harasawa, R., Zanetti, A., 2008b. Taxonomy of Genus *Hepacivirus*. Application of palindromic nucleotide substitutions for the determination of genotypes of human hepatitis C virus species. J. Virol. Methods 153, 280–299.

Harasawa, R., Giangaspero, M., 1998. A novel method for pestivirus genotyping based on palindromic nucleotide substitutions in the 5′-untranslated region. J. Virol. Methods 70, 225–230.

Kirkland, P.D., Frost, M.J., Finlaison, D.S., King, K.R., Ridpath, J.F., Gu, X., 2007. Identification of a novel virus in pigs-Bungowannah virus: a possible new species of pestivirus. Virus Res. 129 (1), 26–34.

Liu, L., Kampa, J., Belák, S., Baule, C., 2009a. Virus recovery and full-length sequence analysis of atypical bovine pestivirus Th/04_KhonKaen. Vet. Microbiol. 138, 62–68.

Liu, L., Xia, H., Wahlberg, N., Belák, S., Baule, C., 2009b. Phylogeny, classification and evolutionary insights into pestiviruses. Virology 385, 351–357.

Oguzoglu, T.C., Tan, M.T., Toplu, N., Demir, A.B., Bilge-Dagalp, S., Karaoglu, T., Ozkul, A., Alkan, F., Burgu, I., Haas, L., Greiser-Wilke, I., 2009. Border disease virus (BDV) infections of small ruminants in Turkey: a new BDV subgroup? Vet. Microbiol. 135, 374–379.

Plowright, W., 1969. Other virus diseases in relation to the JP15 programme. In: Joint Campaign Against Rinderpest. Proceedings of the 1st technical review meeting, phase IV, Mogadiscio , Organization of African Unity, Kenya, pp. 19–23.

Schirrmeier, H., Strebelow, G., Depner, K., Hoffmann, B., Beer, M., 2004. Genetic and antigenic characterization of an atypical pestivirus isolate, a putative member of a novel pestivirus species. J. Gen. Virol. 85 (12), 3647–3652.

Thabti, F., Letellier, C., Hammami, S., Pepin, M., Ribiere, M., Mesplede, A., Kerkhofs, P., Russo, P., 2005. Detection of a novel border disease virus subgroup in Tunisian sheep. Arch. Virol. 150 (2), 215–229.

Valdazo-Gonzalez, B., Alvarez-Martinez, M., Greiser-Wilke, I., 2006. Genetic typing and prevalence of Border disease virus (BDV) in small ruminant flocks in Spain. Vet. Microbiol. 117 (2–4), 141–153.

Valdazo-Gonzalez, B., Alvarez-Martinez, M., Sandvik, T., 2007. Genetic and antigenic typing of border disease virus isolates in sheep from the Iberian Peninsula. Vet. J. 174 (2), 316–324.

Vilček, S., Herring, J.A., Nettleton, P.F., Lowings, J.P., Paton, D.J., 1994. Pestiviruses isolated from pigs, cattle and sheep can be allocated into at least three genogroups using polymerase chain reaction and restriction endonuclease analysis. Arch. Virol. 136, 309–323.

Vilček, S., Paton, D.J., Durkovic, B., Strojny, L., Ibata, G., Moussa, A., Loitsch, A., Rossmanith, W., Vega, S., Scicluna, M., Palfi, V., 2001. Bovine viral diarrhoea virus genotype 1 can be separated into at least eleven genetic groups. Arch. Virol. 146, 99–115.

Vilček, S., Ridpath, J.F., Van Campen, H., Cavender, J.L., Warg, J., 2005. Characterization of a novel pestivirus originating from a Pronghorn antilop. Virus Res. 108, 187–193.

Xu, X., Zhang, Q., Yu, X., Liang, L., Xiao, C., Xiang, H., Tu, C., 2006. Sequencing and comparative analysis of a pig bovine viral diarrhea virus genome. Virus Res. 122 (1–2), 164–170.

Zuker, M., Stiegler, P., 1981. Optimal computer folding of large RNA sequences using thermodynamics and auxiliary. Nucleic Acids Res. 9, 133–148.

NOTE *Bacteriology*

Molecular Identification of '*Candidatus* Mycoplasma haemovis' in Sheep with Hemolytic Anemia

Jin SUZUKI[1)], Fumina SASAOKA[1)], Masatoshi FUJIHARA[1)], Yusaku WATANABE[1)], Tomoko TASAKI[2)], Shinichi ODA[2)], Saori KOBAYASHI[3)], Reeko SATO[3)], Kazuya NAGAI[4)] and Ryô HARASAWA[1)]*

Departments of [1)]Veterinary Microbiology, [2)]Animal Science, [3)]Veterinary Internal Medicine and [4)]Cryobiofrontier Research Center, Faculty of Agriculture, Iwate University, Morioka 020–8550, Japan

(Received 10 March 2011/Accepted 12 April 2011/Published online in J-STAGE 26 April 2011)

ABSTRACT. We examined the presence of hemoplasmas, hemotropic mycoplasmas, among 11 sheep (*Ovis aries*) with regenerative and hemolytic anemia and found six of them were positive by real-time PCR. The positive samples were then subjected to conventional PCR for direct sequencing of the 16S rRNA gene. Nucleotide sequences of all the positive samples were identified as the 16S rRNA gene of '*Candidatus* Mycoplasma haemovis' by phylogenetic analysis, demonstrating the infections with this particular hemoplasma species in Japan.

KEY WORDS: hemoplasma, mycoplasma, ovine, rRNA, sheep.

J. Vet. Med. Sci. 73(8): 1113–1115, 2011

Hemoplasmas are tiny epierythrocytic prokaryotes that lack a cell wall like other mycoplasmas and are susceptible to tetracyclines, but have never been cultured *in vitro*. Infections may lead to hemolytic anemia in animals, but veterinary investigation had been hampered by the lack of appropriate diagnostic procedures. Although most studies relied on cytological identification of the organisms on blood smears, this method has a low diagnostic sensitivity and cannot differentiate the species [4]. Besides, this diagnostic method may misidentify the hemoplasmas as Howell-Jolly bodies, since the both appear frequently after splenectomy, associate with anemia, and contain DNA. Currently only two hemoplasma species, *Mycoplasma ovis* (previously known as *Eperythrozoon ovis*) [5] and '*Candidatus* Mycoplasma haemovis' [3] are recognized in sheep (*Ovis aries*). Although *M. ovis* infection among sheep is prevalent throughout the world, '*Candidatus* M. haemovis' has not been detected in Japan so far. In the present study we investigated an outbreak of infection with '*Candidatus* M. haemovis' in anemic sheep on an experimental farm in Iwate University, Morioka (latitude 39.7N and longitude 141.1E), Japan.

The disease manifested between October and December of 2010, and mainly affected yearlings, which were purchased from a commercial farm in the Iwate prefecture. Hematological examination was carried out on 11 animals with mild regenerative anemia and blood smears were prepared for Giemsa staining. Small, coccoid, epicellular parasites were detected on erythocytes by microscopic examination of the Giemsa-stained blood smears (Fig. 1). Hematocrit, hemoglobin, and red blood cells values of these animals were 9.6 to 25.7%, 2.5 to 7.1 g/d*l*, and 350 to 800 × 10^4/d*l*, respectively, being below the normal ranges.

Total DNA was extracted from 200 μl EDTA-anticoagulated blood samples collected from sheep using the QIAamp DNA Blood Mini Kit (Qiagen, Hilden, Germany) according to the manufacturer's instructions. Negative controls consisting of 200 μl phosphate-buffered saline were prepared with each batch. Extracted DNA samples were stored at –20°C prior to use. To detect the hemoplasmas in real-time PCR, specific primers for the 16S rRNA gene were originally designed. Forward primer Hemo-F, 5'-TCCATA TTCCTACGGGAAGCAA-3', and reverse primer Hemo-R, 5'-TACCCCTTGATTAACTCTAA-3'. Real-time PCR was performed in a SmartCycler instrument (Cepheid, Sunnyvale, CA, U.S.A.) with SYBR Premix Ex *Taq* (Code #RR041A, TaKaRa Bio, Shiga, Japan). The reaction mixture contained 1 μl of each primer (10 pmol/μl), 12.5 μl of

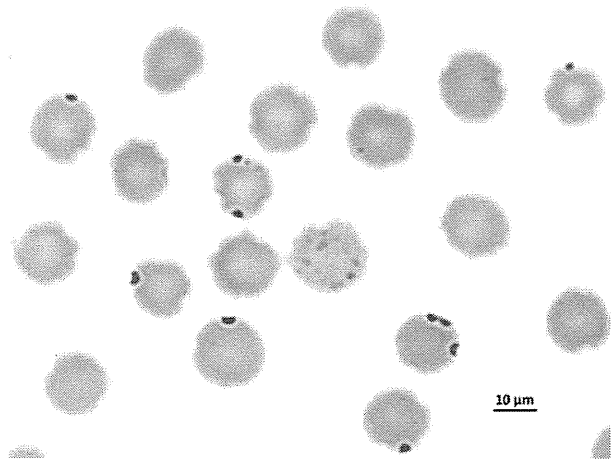

Fig. 1. Giemsa-stained blood smear from an affected sheep with '*Candidatus* M. haemovis'. Hemotrophic mycoplasma cells were seen on the surface of erythrocytes.

* CORRESPONDENCE TO: HARASAWA, R., Department of Veterinary Microbiology, Faculty of Agriculture, Iwate University, Morioka 020–8550, Japan.
e-mail: harasawa-tky@umin.ac.jp

2× premix reaction buffer and water to volume of 23 μl. Finally, 2 μl of DNA samples as templates were added to this mixture. Amplification was achieved with 40 cycles of denaturation at 95°C for 5 sec, renaturation at 57°C for 20 sec, and elongation at 72°C for 15 sec, after the initial denaturation at 94°C for 30 sec. Fluorescence readings in a channel for SYBR Green I were taken throughout the experiments.

After real-time PCR, melting experiment was performed from 60 to 95°C at 0.2°C/sec with smooth curve setting averaging one point. Melting peaks were visualized by plotting the first derivative against the melting temperature (*Tm*) as described previously [2]. The *Tm* was defined as a peak of the curve, and if the highest point was a plateau, then the mid-point was identified as the *Tm*. The input amount of DNA, the copy number of the target as well as presence of co-infections with several targets did not influence the *Tm*. Since nucleotide sequences and sizes bracketed by the primers are specific to species, melting curve analysis of the amplified products may serve as a differential marker for hemoplasma speciation. Six ovine blood samples, Hitsuji1, Hitsuji5, Hitsuji6, Hitsuji7, Hitsuji8 and Hitsuji9, were positive in the real-time PCR. The *Tm* (mean ± SE.) values of the PCR products from these six ovine hemoplasma were estimated to 83.60 ± 0.09°C (Fig. 2).

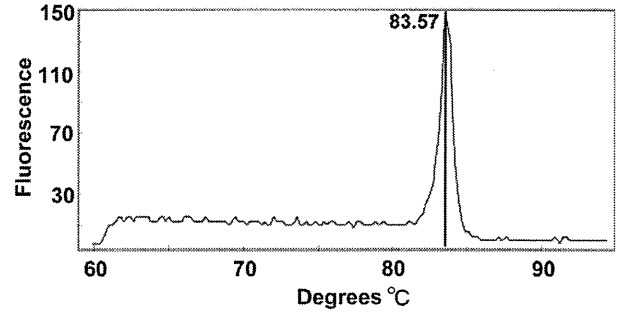

Fig. 2. Thermal melting curve of the PCR products depicted by using SYBR Green I. A characteristic melting temperature at 83.57°C was evident in '*Candidatus* M. haemovis' infection.

The positive samples were further examined by conventional PCR targeting the 16S rRNA gene for nucleotide sequencing. The conventional PCR was carried out with 50-

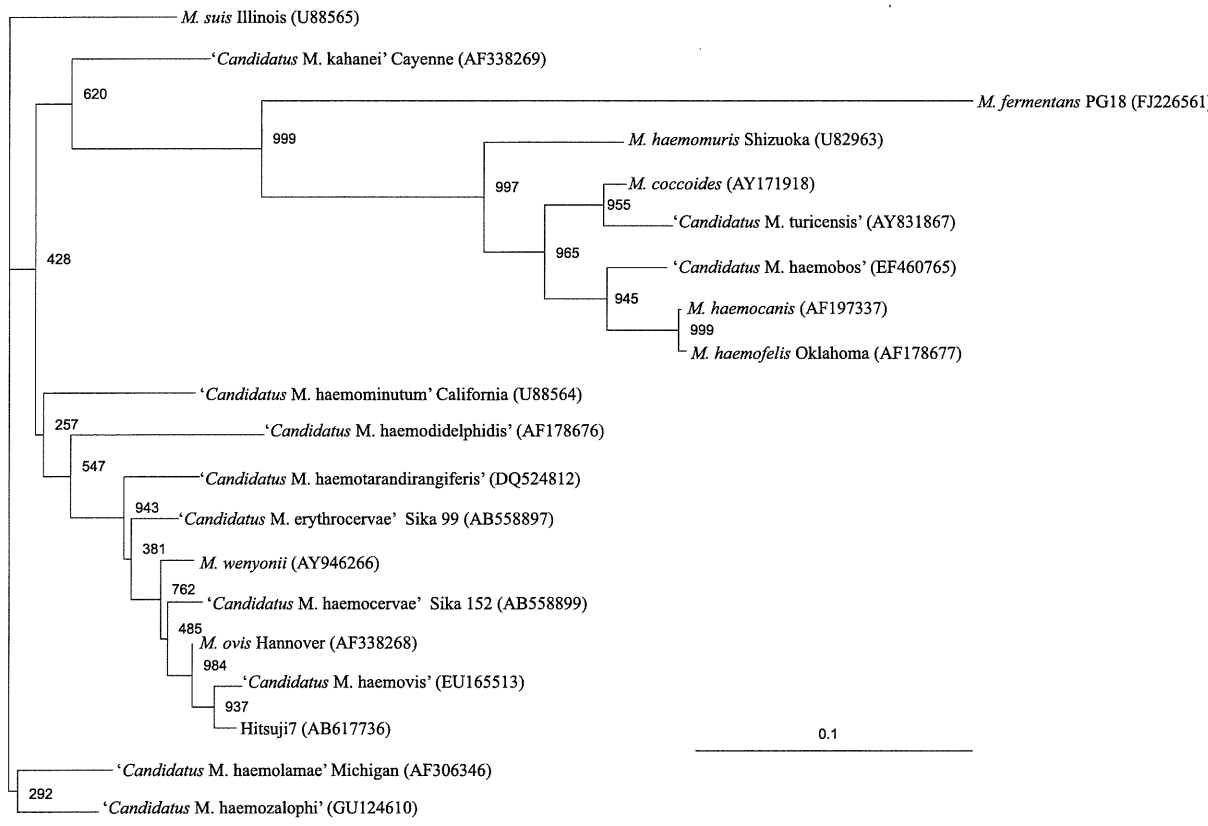

Fig. 3. A phylogenetic tree based on the 16S rRNA gene sequence comparison among mycoplasmas including 18 hemoplasma species (accession numbers are given in a parenthesis). Genetic distances were computed with CLUSTAL W [9]. Ovine strain Hitsuji7 representing Hitsuji1, Hitsuji5, Hitsuji6, Hitsuji8 and Hitsuji9 was included in the '*Candidatus* M. haemovis' clade. A nucleotide sequence of the 16S rRNA gene of *M. fermentans* PG18 strain with accession number FJ226561 was included as an out-group. Numbers in the relevant branches refer to the values of boot-strap probability of 1,000 replications. Scale bar indicates the estimated evolutionary distance.

μl reaction mixtures containing 1 μl of DNA solution, 0.5 μl of TaKaRa LA *Taq* ™ (5 units/μl), 5 μl of 10X LA PCR™ Buffer II, 8 μl of 25 mM $MgCl_2$ (final 4.0 mM), 8 μl of dNTP mixture (2.5 mM each), 0.2 μl (50 pmol/μl) of forward primers Ana-F1 (5'-GAGTTTGATCCTGGCTCAGG-3') or Hemo-F10 (5'- ATATTCCTACGGGAAGC AGC-3'), 0.2 μl (50 pmol/μl) of reverse primers Hemo-R11 or Hemo-R2 (5'-TACCTTGTTACGACTTAACT-3') and water to a final volume of 50 μl. After the mixture was overlaid with 20 μl of mineral oil, the reaction cycle was carried out 35 times with denaturation at 94 for 30 sec, annealing at 60 for 120 sec and extension at 72 for 60 sec in a thermal cycler.

The PCR products were fractionated on horizontal, submerged 1.0% SeaKem ME agarose gels (FMC Bioproducts, Rockland, ME., U.S.A.) in TAE (40 mM Tris, pH8.0, 5 mM sodium acetate, 1 mM disodium ethylenediaminetetracetate) buffer at 50 volts for 60 min. After electrophoresis, the gels were stained in ethidium bromide solution (0.4 μg/m*l*) for 15 min and visualized under UV transilluminator. DNA was extracted by using NucleoSpin Extract II kit (Macherey-Nagel, Düren, Germany) and was subjected to direct sequencing in a 3500 Genetic Analyzer (Applied Biosystems, Foster City, CA, U.S.A.). In our experiments, results between the real-time PCR and conventional PCR were always consistent. The nucleotide sequences of the partial 16S rRNA gene have been deposited in the DDBJ, EMBL, GSDB and NCBI nucleotide sequence databases under the accession numbers AB617733 to AB617738. A single nucleotide substitution was apparent among these six sequences, suggesting a same lineage.

Nucleotide sequences of the 16S rRNA gene from the ovine strain along with the 19 established mycoplasma species were aligned using CLUSTAL W (version 1.83; DDBJ, Mishima, Japan) with further adjustment made manually by eyes as necessary [9]. A phylogenetic tree constructed by the algorithms implemented in the PHYLIP program (DDBJ, Japan) using the neighbor-joining method [7] indicated that the hemoplasma strain detected in sheep was classified as '*Candidatus* Mycoplasma haemovis' (Fig. 3). Besides, the nucleotide sequence '*Candidatus* M. haemovis' detected in the present study were most closely to *Mycoplasma* sp. TX1294-A (accession number GU230141) and TX1294-E (accession number GU383116) strains both detected from humans [8], suggesting an anthropozoonotic pathogen.

'*Candidatus* M. haemovis' was first demonstrated from a sheep flock with fatal hemolytic anemia in Hungary [3]. Prevalence of this hemoplasma species is currently unknown, because there has been no report on this particular species in other countries though *M. ovis* is prevalent throughout the world [1, 6]. We demonstrated this hemoplasma species in anemic sheep in Japan. Variations in the hematological values might be attributed to infection stages rather than differences in the hemoplasma strains, which were almost identical in the 16S rRNA sequences. It is most likely that the animals had been infected in the commercial farm, since the affected sheep in the present study was the only flock in the experimental farm of the Iwate University.

REFERENCES

1. Aguirre, D. H., Thompson, C., Neumann, R. D., Salatin, A. O., Gaido, A.B . and Torioni de Echaide, S. 2009. Brote de micplasmosis clinica por *Mycoplasma ovis* en ovinos de Salta, Argentina. Diagnostico clinico, microbiologico y molecular. *Rev. Argentina Microbiol.* **41**: 212–214.
2. Harasawa, R., Mizusawa, H., Fujii, M., Yamamoto, J., Mukai, H., Uemori, T., Asada, K. and Kato, I. 2005. Rapid detection and differentiation of the major mycoplasma contaminants in cell cultures using real-time PCR with SYBR Green I and melting curve analysis. *Microbiol. Immunol.* **49**: 859–863.
3. Hornok, S., Meli, M. L., Erdos, A., Hajtos, I., Lutz, H. and Hofmann-Lehmann, R. 2009. Molecular characterization of two different strains of haemotropic mycoplasmas from a sheep flock with fatal haemolytic anaemia and concomitant *Anaplasma ovis* infection. *Vet. Microbiol.* **136**: 372–377.
4. Messick, J. B. 2004. Hemotrophic mycoplasmas (hemoplasmas): a review and new insights into pathogenic potential. *Vet. Clin. Pathol.* **33**: 2–13.
5. Neimark, H., Hoff, B. and Ganter, M. 2004. *Mycoplasma ovis* comb. nov. (formerly *Eperythrozoon ovis*), an epierythrocytic agent of haemolytic anaemia is sheep and goats. *Int. J. Syst. Evol. Microbiol.* **54**: 365–371.
6. Ohtake, Y., Nishizawa, I., Sato, M., Watanabe, Y., Nishimura, T., Matsubara, K., Nagai, K. and Harasawa, R. 2011. *Mycoplasma ovis* detected in free-living Japanese serows, *Capricornis crispus*. *J. Vet. Med. Sci.* **73**: 371–373.
7. Saitou, N. and Nei, M. 1987. The neighbor-joining method: a new method for reconstructing phylogenetic trees. *Mol. Biol. Evol.* **4**: 406–425.
8. Sykes, J. E., Lindsay, L. L., Maggi, R.G . and Breitschwerdt, E. B. 2010. Human co-infection with *Bartonella henselae* and two hemotropic mycoplasma variants resembling *Mycoplasma ovis*. *J. Clin. Microbiol.* **48**: 3782–3785
9. Thompson, J. D., Higgins, D. G. and Gibson, T. J. 1994. CLUSTAL W: improving the sensitivity of progressive multiple sequence alignment through sequence weighting, position-specific gap penalties and weight matrix choice. *Nucleic Acids Res.* **22**: 4673–4680.

Microbiology and Immunology

Microbiol Immunol 2011; **55**: 489–493
doi:10.1111/j.1348-0421.2011.00345.x

ORIGINAL ARTICLE

Acidic environments induce differentiation of *Proteus mirabilis* into swarmer morphotypes

Masatoshi Fujihara[1,2], Hisato Obara[1,2], Yusaku Watanabe[1,2], Hisaya K. Ono[2], Jun Sasaki[2,3], Masanobu Goryo[2,3], and Ryô Harasawa[1,2]

[1]Department of Veterinary Microbiology, Faculty of Agriculture, Iwate University, [2]Department of Applied Veterinary Science, United Graduate School of Veterinary Science, Gifu University, Gifu, Japan, and [3]Department of Veterinary Pathology, Faculty of Agriculture, Iwate University, Iwate

ABSTRACT

Although swarmer morphotypes of *Proteus mirabilis* have long been considered to result from surfaced-induced differentiation, the present findings show that, in broth medium containing urea, acidic conditions transform some swimmer cells into elongated swarmer cells. This study has also demonstrates that *P. mirabilis* cells grown in acidic broth medium containing urea enhance virulence factors such as flagella production and cytotoxicity to human bladder carcinoma cell line T24, though no significant difference in urease activity under different pH conditions was found. Since there is little published data on the behavior of *P. mirabilis* at various hydrogen-ion concentrations, the present study may clarify aspects of cellular differentiation of *P. mirabilis* in patients at risk of struvite formation due to infection with urease-producing bacteria, as well as in some animals with acidic or alkaline urine.

Key words cytotoxicity, hydrogen-ion, *Proteus mirabilis*, swarmer cell.

Proteus species, Gram-negative bacteria in the family *Enterobacteriaceae*, cause urinary tract infections. Affected patients with long-term urinary catheters in place or structural abnormalities of the urinary tract have an increased risk of struvite and carbonate apatite formation, due to increase in their urinary pH and direct damage to the uroepithelium by ammonia (1–3). *Proteus* infections are frequently persistent and difficult to treat and can lead to complications such as acute or chronic pyelonephritis. Additionally, *Proteus* species are the most common bacilli associated with the formation of bacteria-induced bladder and kidney stones (about 70% of all bacteria isolated from such urinary calculi) (4, 5).

Proteus mirabilis may also form a bull's-eye pattern on an agar plate because it sometimes swarms over the entire surface of the agar medium. Differentiation into swarmer cells, which are characterized by a 10 to 40-fold increase in cell length, a drastic increase in the number of flagella and production of higher amounts of specific virulence factors, is considered to be closely related to establishment of infections (6, 7). Swarmer cell differentiation is initiated upon contact with a solid surface, by inhibition of flagellar rotation, or by cell–cell signaling (8–11), but *P. mirabilis* is usually unable to differentiate into swarmer cells on minimal media (12). Jones *et al.*, however, have reported that biofilms in artificial urine (pH 6.5) produce greater numbers of swarmer cell populations than those observed in Luria broth, and suggested that swarmer cells have an important role in urinary tract biofilms (13). In this study, we found that broth cultures containing urea under acidic conditions induced a few swarmer morphotypes of *P. mirabilis* L1N2.

Correspondence
Ryô Harasawa, Department of Veterinary Microbiology, Faculty of Agriculture, Iwate University, Morioka, Iwate 020-8550, Japan. Tel/Fax: +81196216158; email: harasawa@iwate-u.ac.jp

Received 23 July 2010; revised 15 March 2011; accepted 1 April 2011.

List of Abbreviations: DAPI, 4′,6-diamidino-2-phenylindole; HBSS, Hanks' balanced salt solution; HEPES, 4-(2-hydroxyethyl)-1-piperazineethanesulfonic acid; LDH, lactate dehydrogenase; *P. mirabilis Proteus mirabilis*; SE, standard error; T5, 7 or 9, Trypto-soy broth pH 5, 7 or 9; UT5, 7 or 9, urea containing Trypto-soy broth pH 5, 7 or 9.

Little is known about the behavior of *P. mirabilis* in alkaline urine in patients infected with urease producing bacteria. Moreover, urinary pH varies among animal species. For example, carnivores void acidic urine (*Felis catus*: pH 5~7) but herbivores void alkaline urine (*Bos taurus*: pH 7~9). Although *P. mirabilis* is mainly a human uropathogen, it also infects the urinary tracts of carnivores and other omnivores. In contrast, infections of the urinary tract of herbivores are rare, though *P. mirabilis* has been isolated from the respiratory and genital tracts of cattle (14, 15). Therefore, in the present study, we examined the behavior of *P. mirabilis* L1N2 at several pHs of Trypto-soy broth with or without urea.

MATERIALS AND METHODS

Bacterial strain and growth conditions

Proteus mirabilis strain L1N2, kindly supplied by Professor S. Igimi of the National Institute of Health Sciences in Tokyo, was grown in Trypto-soy broth or agar (Eiken Chemical, Tokyo, Japan). Trypto-soy broth was adjusted to pH 5.0, 7.0 or 9.0, supplemented with 25 g/L urea (designated UT5, UT7 or UT9, respectively) or without urea (T5, T7 or T9, respectively), and filter-sterilized. Because growth rates vary according to the pH conditions, bacterial numbers were adjusted by inoculating about 10^5, 10^2 or 10^3 bacterial cells into 1 mL broth at pH 5.0, 7.0 or 9.0, and incubating them at 37°C for 12 hr. For controls, swarmer cells were harvested with a platinum loop from the margins of colonies grown on Trypto-soy agar at 37°C and suspended in PBS. Bacterial cells were harvested from the bacterial suspension by centrifugation at 12,000 × *g* for 1 min and used for the following experiments.

Cell morphology

Bacterial cells collected by centrifugation were resuspended to a concentration of $10^{9\sim10}$/mL in PBS containing 1 μg/mL of FM1–43FX (Invitrogen, Eugene, OR, USA) and 2 μg/mL of DAPI (Dojindo, Kumamoto, Japan). The bacterial cells were examined with an Eclipse TE2000-U fluorescence microscope (Nikon, Tokyo, Japan) with mercury lamp. Fluorescent signals were observed by using the phase contrast objective UplanF1100X and a U-WIBA filter cube (an FM1–43 excitation filter for 460–490 nm and a barrier filter for 515–550 nm) or a U-NUA filter cube (a DAPI excitation filter for 360–370 nm and a barrier filter for 420–460 nm). Images were captured and submerged by using a VB-7010 digital camera (Keyence, Osaka, Japan). Bacterial cells longer than 10 μm were defined as swarmer morphotypes (16).

Bacterial flagella were observed with an H-800 transmission electron microscope (Hitachi, Tokyo, Japan). Aliquots of bacterial suspension fixed with 10% neutral-buffered formalin, were placed on a formvar-coated grid and negatively stained with 1% uranyl acetate.

Urease activity

Bacterial cells washed twice with 50 mM HEPES buffer (pH 7.5) and sonicated on ice to release soluble proteins served as a crude urease preparation. Following centrifugation at 12,000 × *g* for 2 min, the supernatant fluids were placed on ice. The concentrations of the crude enzyme extracts were determined by Coomassie brilliant blue protein assay solution (Nacalai, Kyoto, Japan), according to the manufacturer's protocol. BSA was used as a standard.

The urease activity of the extracts was estimated by measuring the amount of ammonia molecules released from urea in a phenol-hypochlorite assay (17). Briefly, the extracts were added to the urease buffer (50 mM HEPES buffer, pH 7.5, plus 25 mM urea) in a 330 μL final volume and incubated at 37°C for 20 min. The reaction was stopped by adding to a cuvette with 500 μL of solution A (containing 10 g of phenol and 50 mg of sodium nitroprusside per liter). An equal volume (500 μL) of solution B consisting of 5 mg/mL NaOH and 0.044% (v/v) NaClO was added and mixed well. Following incubation at 37°C for 30 min, the absorbance at 625 nm was measured in a Bio-Spec-mini spectrophotometer (Shimadzu Scientific Instruments, Kyoto, Japan). Ammonium chloride was used as a standard to convert the absorbance at 625 nm to nanomoles of ammonia. The specific activity of urease was defined as mm of ammonia produced per min per mg of protein. Values were expressed as the mean ± SE of four to five independent cultures in triplicate assays.

Cytotoxicity assay

A transitional human bladder carcinoma cell line T24 obtained from the Japanese Collection of Research Bioresources (Osaka, Japan) was routinely maintained in Dulbecco's modified Eagle medium (Nissui, Tokyo, Japan) supplemented with 10% FBS (Invitrogen), 2 mM glutamine and penicillin/streptomycin (50 U/mL and 50 μg/mL) at 37°C in a humidified 5% carbon dioxide atmosphere. Cytotoxicity was examined by using the Cytotoxicity Detection Kit (Roche Applied Science, Indianapolis, IN, USA) which measures LDH release from the cytosol of damaged T24 cells into the supernatant fluids. Two controls were included for calculation of the cytotoxicity rate (%). Low controls consisted of supernatant fluids from T24 cells with no exposure to bacteria. High controls were from cells treated with lysis solution for 15 min. LDH activity was examined three times in a 96-wells plate, according to the manufacturer's protocol. Cultured cells were infected with about 1.0×10^6

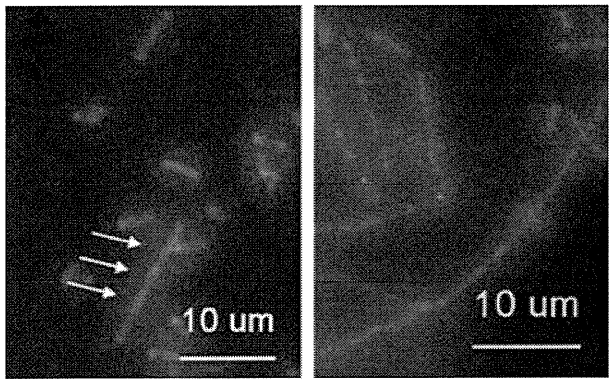

Fig. 1. DAPI and FM1-43FX staining of bacterial cells grown in UT5 (left hand photo)and on agar plates (right hand photo). These photos depict elongated multinuclear cells (arrows in UT5).

($0.7 \sim 1.5 \times 10^6$) of *P. mirabilis* grown in each medium for 30 min in incubation solution (HBSS- minimal medium-0.2M Tris buffer, pH 7.5, 80:10:10% v/v) as described by Peerbooms *et al.* (18). Cytotoxicity was expressed as the mean percentage ([experimental value–low control]/[high control–low control] $\times$ 100 $\pm$ SE) for three independent examinations.

Statistical analysis

All values are presented as the mean $\pm$ SE. Statistical analysis was performed by JMP software (SAS Institute, Cary, NC, USA) using one-way analysis of variance followed by the Turkey-Kramer test.

RESULTS

Cell morphology

The final pH values of broth media T5, T7, T9, UT5, UT7 and UT9 were 4.9, 6.0, 8.0, 8.7, 9.2 and 9.2, respectively. The percentage of swarmer morphotypes was 0.6% in T5, 0.2% in T7, less than 0.1% in T9, 1.8% in UT5, 0.8% in UT7 and 0.1% in UT9. Swarmer morphotypes appeared in acidic rather than alkaline broth, irrespective of the addition of urea. Elongated and multinucleated cells grown in broth media, which were morphologically similar to swarmer cells grown on agar plates, were stained with DAPI (Fig. 1). More than 70% of the *P. mirabilis* L1N2 cells on agar plates were longer than 10 μm. Two other *P. mirabilis* strains, NBRC 3849 and NBRC 105697, both purchased from the National Institute Technology and Evaluation (Osaka, Japan), behaved similarly, the incidence of swarmer morphotypes of these two strains in broth cultures without urea being less than 0.1%. The incidence of swarmer morphotypes of NBRC 3849 was 1.1, 0.3 and 0.1% in UT5, UT7 and UT9, respectively. Similarly, the incidence of swarmer morphotypes of NBRC105697 was 2.6, 1.2 and 0.4% in UT5, UT7 and UT9, respectively.

Electron microscopic photos of bacterial cells grown in each broth are shown in Figure 2. Elongated and hyperflagellated cells, as well as short swimmer cells expressing many flagella, were evident in UT5. Similarly, bacterial cells grown in T7, T9 and UT7 also expressed peritrichous flagella. The number of flagella on bacterial cells grown in T5 and UT9 was markedly decreased.

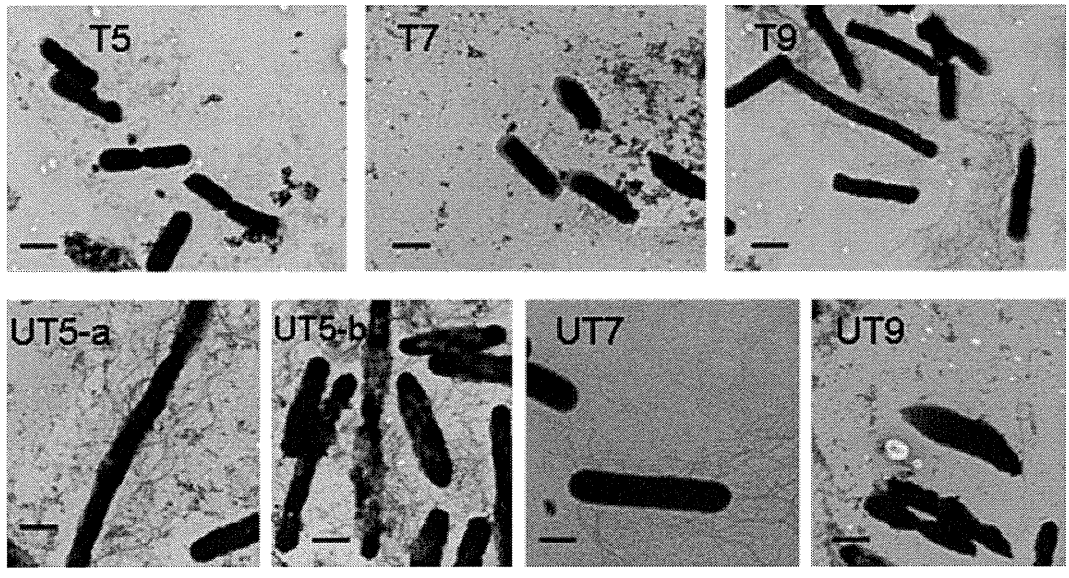

Fig. 2. Electron micrographs of bacterial cells grown in each broth. Many peritrichous flagella are visible on the elongated cells (UT5-a) and short rods (UT5-b) in UT5. The bacterial cells in T7, T9 and UT7 are also expressing peritrichous flagella, but those in T5 and UT9 show small number of flagella. Bar represents 1 μm.

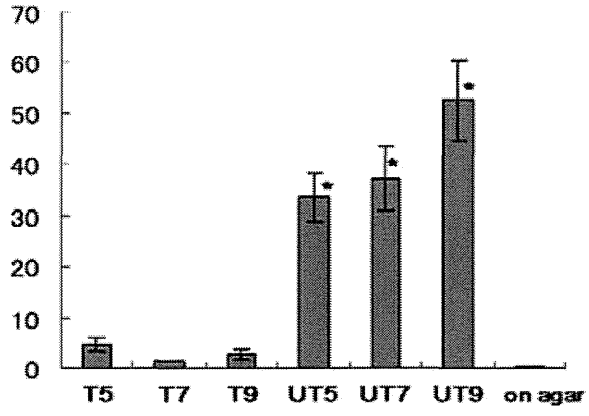

Fig. 3. Urease activities in each broth and on agar plates. The specific activity of urease was defined as μ mol of ammonia produced /min/mg of protein. Values are expressed as the mean ± SE for four to five independent cultures, with each assay made in triplicate. Asterisks shown above the columns indicate a significant difference from the cells grown in T5, T7, T9 and on agar plates ($P < 0.05$).

Urease activity

Urease activities for each broth and agar medium are shown in Figure 3. Urease activities in broth containing urea were around tenfold higher than in broth without urea, but no significant change was evident in broths of different pH. Urease activities (expressed as μmol of ammonia/min/mg of protein) in the broth media were 4.72 ± 1.47 (mean ± SE) in T5, 1.34 ± 0.13 in T7, 2.75 ± 1.20 in T9, 32.34 ± 5.94 in UT5, 33.45 ± 6.70 in UT7, 52.26 ± 10.11 in UT9. The urease activity in swarmer cells grown on agar plates was 0.26 ± 0.06.

Cytotoxicity

Results of cytotoxicity tests are shown in Figure 4. Swarmer cells on agar palates showed the highest cytotoxicity (90.56 ± 1.29% [mean ± SE]). Bacterial cells grown in UT5 showed 11.12 ± 0.17% cytotoxicity, whereas cells grown in the other broths showed less than 5% cytotoxicity (the high controls were taken as 100%).

DISCUSSION

Infections by urease-producing bacteria increase urinary pH due to hydrolysis of urea into carbon dioxide and ammonia. During the process of infection, the alkaline environment might increase the pathogenicity of *P. mirabilis*. For example, the optimum pH for subtilase-like protease activity in toxic agglutinin is 8.5–9.0, which is also optimal for expression of toxic agglutinin encoded by PMI2341 of *P. mirabilis* (19). However, in the present studies, 1.8% of cells of *P. mirabilis* L1N2 grown in UT5 differentiated into hyperflagellated swarmer morphotypes, thus enhancing cytotoxicity, though the inoculum size was changed because of the slow growth rate in UT5, and the pH was increased by urease activity after 12 hr of incubation. On the other hand, shorter rods appeared in UT9; these were less flagellated and had lower cytotoxicity. The cytotoxicity of the other strains, NBRC 3849 and NBRC 105697, in UT5 was also higher than in other broth media (data not shown). These results pose questions about the optimum pH for expression of other virulence factors and swarmer cell differentiation.

Differentiation into swarmer cells is considered to be linked to expression of virulence factors such as hemolysin and IgA metalloprotease (20, 21). Hemolysin activity is known to be responsible for the cytotoxicity of *P. mirabilis* (22). Urease activity, which we did not examine, is also increased during swarming on urea-containing agar plates (6). Further examination is necessary to confirm the virulence of swarmer cells and their temporal behavior *in vivo*, since swimmer morphotypes have predominantly been previously demonstrated in mouse models of ascending urinary-tract infection (16). Our results suggest that *P. mirabilis* cells differentiate into swarmer morphotypes at an early phase of infection when the host's urine is acidic, but they dedifferentiate into swimmer morphotypes when the urinary pH is increased.

Allison *et al.* have reported that the swarming phenomenon of *P. mirabilis* is responsible for the ability to invade into Vero cells and two human uroepithelial cell lines (22). They showed that swarmer cells invade within

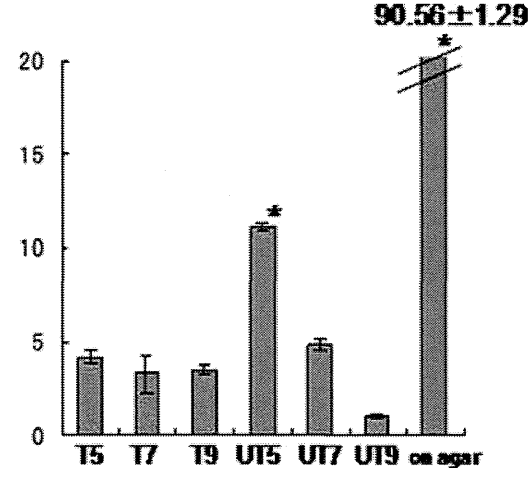

Fig. 4. Cytotoxicity (%) of *P. mirabilis* cells grown in each broth and on agar plates. LDH activities were determined in triplicate wells of a 96 well plate. High controls were used as a standard (100%) and values are expressed as the mean ± SE for three independent cultures, with each assay made in triplicate. Asterisks shown above the columns indicate a significant difference from the cells grown in other conditions. ($P < 0.05$)

30 mins, the invasion rate being about 15- to 20-fold greater after 2 hr as compared with invasion by swimmer cells, which are internalized more slowly (22). In their study, non-swarming mutants were 25-fold less invasive than wild-type cells. To the contrary, in our study invasion was seen within 30 min in all the broth conditions, though no significant differences were apparent among the broth conditions. The invasive rates of swarmer cells grown on agar plates were not determined because of their high cytotoxicity and detachment of T24 cells (data not shown).

In conclusion, 1.8% cells of *P. mirabilis* L1N2 differentiated into hyperflagellated and multinucleated swarmer morphotypes in acidic broth containing urea, and these cells exerted higher cytotoxicity against T24, though no significant differences were evident in urease activity among the different pH conditions. On the other hand, *P. mirabilis* grown in alkaline broth containing urea showed few elongated cells, and low levels of flagella production and cytotoxicity. Our study may help in the understanding of the cellular differentiation of *P. mirabilis* in the acidic urine of meat eating animals and in the alkaline urine of patients infected with urease producing bacteria or of grass eating animals.

REFERENCES

1. Griffith D.P., Musher D.M., Itin C. (1976) Urease. The primary cause of infection-induced urinary stones. *Invest Urol* **13:** 346–50.
2. Gleeson M.J., Griffith D.P. (1993) Struvite calculi. *Br J Urol* **71:** 503–11.
3. Kramer G., Klingler H.C., Steiner G.E. (2000) Role of bacteria in the development of kidney stones. *Curr Opin Urol* **10:** 35–8.
4. Lerner S.P., Gleeson M.J., Griffith D.P. (1989) Infection stones. *J Urol* **141:** 753–8.
5. Coker, C., Poore, C.A., Li X., Mobley, H.L.T. (2000) Pathogenesis of *Proteus mirabilis* urinary tract infection. *Microbes Infect* **2:** 1497–505.
6. Allison C., Lai H.C., Hughes C. (1992) Co-ordinate expression of virulence genes during swarm-cell differentiation and population migration of *Proteus mirabilis*. *Mol Microbiol* **6:** 1583–91.
7. Allison C., Emody L., Coleman N., Hughes C. (1994) The role of swarm-cell differentiation and multicellular migration in the uropathogenicity of *Proteus mirabilis*. *J Infect Dis* **169:** 1155–8.
8. Rauprich O., Matsushita M., Weijer C.J., Siegert F., Esipov S.E., Shapiro J.A. (1996) Periodic phenomena in *Proteus mirabilis* swarm colony development. *J Bacteriol* **178:** 6525–38.
9. Fraser G.M., Hughes C. (1999) Swarming motility. *Curr Opin Microbiol* **2:** 630–5.
10. Alavi M., Belas R. (2001) Surface sensing, swarmer cell differentiation and biofilm development. *Method Enzymol* **336:** 29–40.
11. Sturgill G., Rather P.N. (2004) Evidence that putrescine acts as an extracellular signal required for swarming in *Proteus mirabilis*. *Mol Microbiol* **51:** 437–46.
12. Sturgill G.M., Siddiqui S., Ding X., Pecora N.D., Rather P.N. (2002) Isolation of *lacZ* fusions to Proteus mirabilis genes regulated by intercellular signaling: potential role for the sugar phosphotransferase (Pts) system in regulation. *FEMS Microbiol Lett* **217:** 43–50.
13. Jones S.M, Yerly J., Hu Y., Ceri H., Martinuzzi R. (2007) Structure of *Proteus mirabilis* biofilms grown in artificial urine and standard laboratory media. *FEMS Microbiol Lett* **268:** 16–21.
14. Decaro N., Campolo M., Desario C., Cirone F., D'Abramo M., Lorusso E., Greco G., Mari V., Colaianni M.L., Elia G., Martella V., Buonavoglia C. (2008) Respiratory disease associated with bovine coronavirus infection in cattle herds in Southern Italy. *J Vet Diagn Invest* **20:** 28–32.
15. Noakes D.E., Wallace L., Smith G.R. (1991) Bacterial flora of the uterus of cows after calving on two hygienically contrasting farms. *Vet Rec* **128:** 440–2.
16. Jansen A.M., Lockatell C.V., Johnson D.E., Mobley H.L.T. (2003) Visualization of *Proteus mirabilis* morphotypes in the urinary tract: the elongated swarmer cell is rarely observed in ascending urinary tract infection. *Infect Immun* **71:** 3607–13.
17. Weatherburn M.W. (1967) Phenol-hypochlorite reaction for determination of ammonia. *Anal Chem* **39:** 971–4.
18. Peerbooms P.G.H., Verweoj A.M.J., MacLaren D.M. (1984) Vero cell invasiveness of *Proteus mirabilis*. *Infect Immun* **43:** 1068–71.
19. Alamuri P., Mobley H.L.T. (2008) A novel autotransporter of uropathogenic *Proteus mirabilis* is both a cytotoxin and an agglutinin. *Mol Microbiol* **68:** 997–1017.
20. Walker K.E., Moghaddame-Jafari S., Lockatell C.V., Johnson D., Belas R. (1999) ZapA, the IgA-degrading metalloprotease of *Proteus mirabilis*, is a virulence factor expressed specifically in swarmer cells. *Mol Microbiol* **32:** 825–36.
21. Fraser G.M., Claret L., Furness R., Gupta S., Hughes C. (2002) Swarming-coupled expression of the *Proteus mirabilis hpmBA* haemolysin operon. *Microbiology* **148:** 2191–201.
22. Allison C., Coleman N., Jones P.L., Hughes C. (1992) Ability of *Proteus mirabilis* to invade human urothelial cells is coupled to motility and swarming differentiation. *Infect Immun* **60:** 4740–6.

NOTE *Bacteriology*

Rapid Identification of Hemoplasma Species by Palindromic Nucleotide Substitutions at the GAAA Tetraloop Helix in the Specificity Domain of Ribonuclease P RNA

Fumina SASAOKA[1)], Jin SUZUKI[1)], Yusaku WATANABE[1,2)], Masatoshi FUJIHARA[1,2)] and Ryô HARASAWA[1,2)]*

[1)]*Department of Veterinary Microbiology, School of Veterinary Medicine, Faculty of Agriculture, Iwate University, Morioka 020–8550 and* [2)]*Department of Applied Veterinary Science, The United Graduate School of Veterinary Sciences, Gifu University, Gifu 501–1193, Japan*

(Received 26 May 2011/Accepted 23 June 2011/Published online in J-STAGE 7 July 2011)

ABSTRACT. We examined secondary structures of the ribonuclease P RNA sequences obtained from DNA databases, and identified a determinative prototype of the P12 helix peculiar to each species of hemoplasmas. This key structure will provide a rapid means for species identification of these uncultivable pathogens without making a phylogenetic tree based on alignments of nucleotide sequences. This procedure based on palindromic nucleotide substitutions at the stem portion of the P12 helix provide clear information such as the level of heterogeneity within a species, the relatedness between species, or facilitating the characterization and clustering of specific strains. In conclusion, the PNS analysis is based on the evaluation of only the strategic and highly conserved genomic region in the specificity domain of RNase P RNA.

KEY WORDS: GAAA tetraloop, hemoplasma, mycoplasma, ribonuclease P RNA.

J. Vet. Med. Sci. 73(11): 1517–1520, 2011

Hemoplasmas, hemotropic mycoplasmas, are causative of infectious anemia not only in animals but also probably in humans [14, 17]. Microbiological identification of hemoplasmas has been hampered by lack of an appropriate means to grow them *in vitro*. Thus the diagnosis of hemoplasma infections has largely been depending on cytological examinations and/or PCR. PCR is most preferably used since the cytological identification of the organisms in blood smear has a low diagnostic sensitivity and may instead detect Howell-Jolly bodies. Only two conserved nucleotide sequences, the 16S rRNA and ribonuclease (RNase) P RNA genes, are widely used in specific PCR diagnosis for hemoplasma infections, and hemoplasmas have been divided into haemominutum and haemofelis clusters based on phylogenetic analyses of these RNA sequences [12]. Although the 16S rRNA gene has long been used for identification and classification of prokaryotes, it is sometimes difficult to distinguish between closely related species, such as *Mycoplasma haemofelis* and *M. haemocanis* [11]. These 2 species have been distinct in the RNase P RNA sequence, though they have been grouped together consistently in phylogenetic analysis of the 16S rRNA sequence [1, 16]. In the present study we found a genetic marker for identification of hemoplasma species by an in-depth investigation of the secondary structure of the RNase P RNA molecules. This genetic marker allows rapid identification of hemoplasma species without aligning nucleotide sequences or making phyologenetic trees.

RNase P RNA, one of the first catalytic RNA molecules, is RNA moiety of RNase P that has been identified in all three domains of life, Bacteria, Eukarya and Archaea [7]. Bacterial RNase P RNA consists of two independently folding domains, a specificity domain and a catalytic domain [9]. The RNase P RNA of mycoplasmas has been assigned to class B architecture represented by *Bacillus subtilis*, including low G+C content Gram-negative bacteria [4]. We have examined the RNase P RNA genes of hemoplasmas and found a useful secondary structure in the specificity domain, that is peculiar to each hemoplasma species. Nucleotide sequences of RNase P RNA were obtained from the DNA databases and referred by accession numbers in the present study.

Prokaryotic RNase P RNA is a ribozyme that is responsible for processing the 5' end of tRNA by cleaving a precursor and leading to tRNA maturation. Several secondary structure modules in RNase P RNA molecules have been predicted from the phylogenetic comparison, which play the interaction with a defined structural motif [15]. The GAAA tetraloop at the top of P12 helix has high affinity for the motif called tetraloop receptor of 11 nucleotides in P10.1 helix of the RNase P RNA class B molecules [8, 10]. *M. fermentans* is the only *Mycplasma* species that lacks the GAAA terminal loop at the P12 helix [13]. Alignments of short nucleotide sequences including the P12 and P10.1 helices of the haemominutum and haemofelis clusters are separately shown in Fig. 1. The GAAA tetranucleotide was conserved at the terminal loop of the P12 helix in all the species of hemoplasmas. Typical 11-nucleotide (5'-TCTAAG.....TATGA-3') motif at the P10.1 portion, that is a putative region for a crossing-pair with the GAAA tetraloop, was well conserved in the haemominutum clusters. Secondary structures of the P12 portions were pre-

* CORRESPONDENCE TO: Prof. HARASAWA, R., Department of Veterinary Microbiology, School of Veterinary Medicine, Faculty of Agriculture, Iwate University, Morioka, Iwate 020–8550, Japan.
e-mail: harasawa-tky@umin.ac.jp

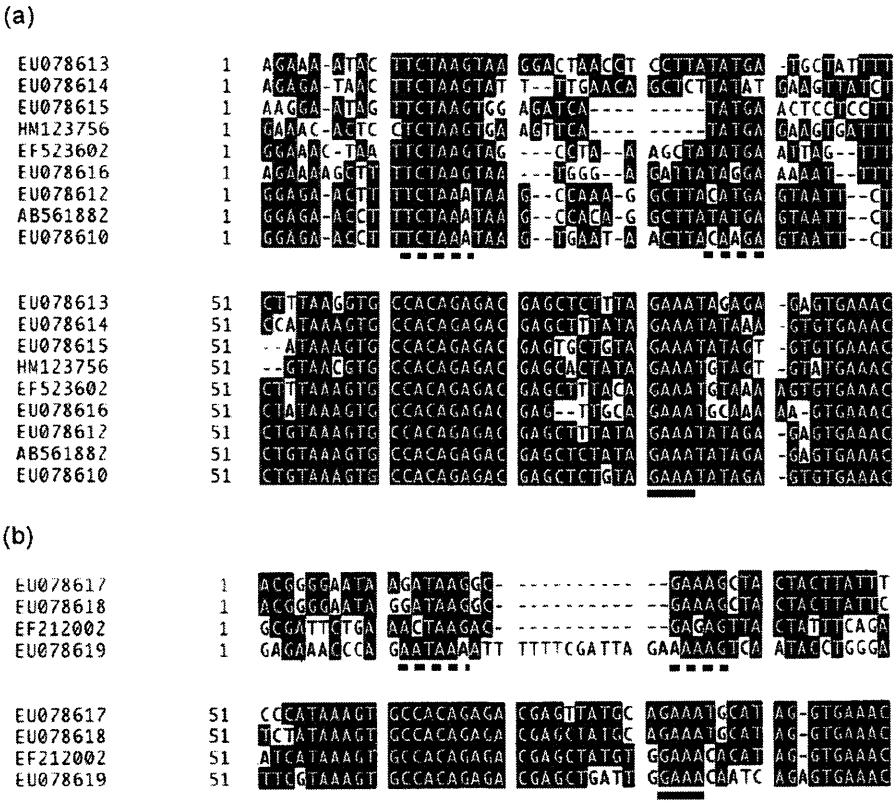

Fig. 1. Nucleotide sequence alignments for partial RNase P RNA genes from the (a) haemominutum and (b) haemofelis clusters in hemoplasmas. Sequences are designated according to accession numbers in the DNA databases as follows, EU078613 for '*Candidatus* M. haemolamae', EU078615 for '*C.* M. kahanei', HM123756 for '*C.* M. aoti', EF523602 for M. suis, EU078616 for '*C.* M. haematoparvum', EU078614 for '*C.* M. haemominutum', EU078612 for *M. ovis*, AB561882 for '*C.* M. haemocervae' EU078610 for *M. wenyonii*, EF 212002 for '*C.* M turicensis', EU078617 for *M. haemofelis*, EU078618 for *M. haemocanis*, and EU078619 for '*C.* M. coccoides'. The GAAA motif at the P12 helix was underlined. Tentative P10.1 portion was marked by a dotted underline. Nucleotides that are identical two out of three sequences are shown as inverted characters. Dashes represent spacers between adjacent nucleotides introduced for maximum matching. The nucleotide numbers are given from a consensus alignment.

dicted according to the algorithm of Zuker and Stiegler [19]. Nucleotide base-pairings at the stem region were variable among hemoplasma species, but capable to form a stable secondary structure to minimize free energy, by G-T wobble as well as canonical Watson-Crick base pairings (Fig. 2). The minimum free energy for the each GAAA tetraloop module was calculated by the method of Freier *et al.* [3]. Size of the stem portion was variable from 5 to 7 base-pairings. Most stems of the P12 helix of hemoplasmas were consisting of seven base-pairings. The shortest stem was appeared in '*Candidatus* M. haematoparvum', but it showed a substantially negative free energy to maintain a stable helix. Sequence divergence at the stem regions was resulted from coordinated mutations of complementary paired nucleotides in base-pairings. Such point mutations, also called palindromic nucleotide substitutions (PNS), may correspond to radical evolutionary changes, and can universally generate new species [2, 5, 6]. The P12 helices of *M. haemofelis* and *M. haemocanis* were almost identical except for a single base-pairing at the inception of the stem structure in terms of PNS. The former showed T-G or T-A pairing at this position but the latter was distinct by transitional substitution, which can be a genetic marker discriminating these two species. Thus, analysis of the secondary structures may provide a clear picture for species identification without making a phylogenetic tree, since nucleotide fluctuation at this particular portion was not found among nine hemoplasma strains (AF407210, AF407212, AY150987, AY150991, DQ859006, DQ859008, DQ859011, EU078611, EU078617) within a single species of *M. haemofelis* (data not shown). The PNS method provides results comparable with other taxonomical procedures by using phylogenetic analysis based on the primary structure, but it differs from them in that only the strategic and highly conserved portions in P12. Point mutations occur continuously and at random through the prokaryotic genome at

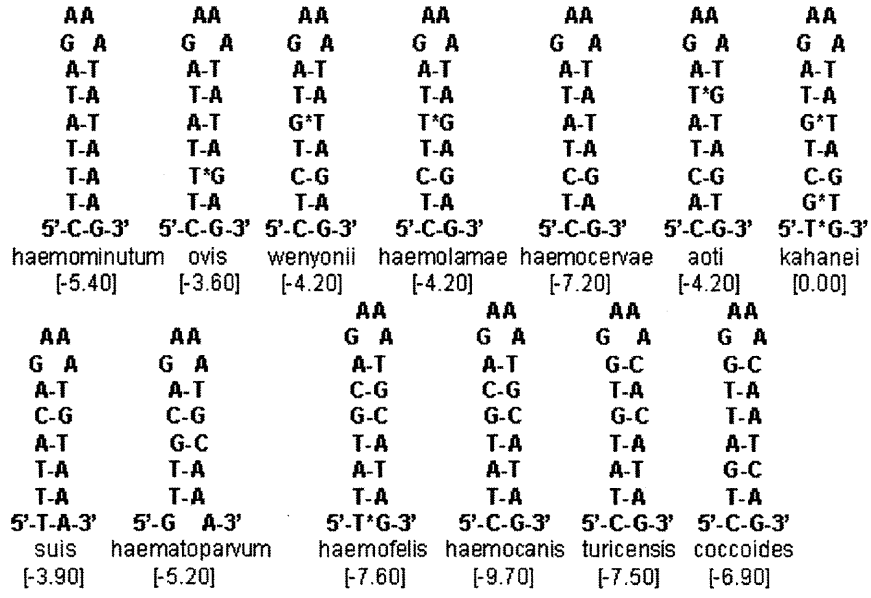

Fig. 2. Secondary structures predicted for the P12 portions in RNase P RNA genes. Watson-Crick base-pairing is indicated by a dash, and a G-T wobble pairing tolerated in the secondary structure by an asterisk. Species designation is shown by specific epithet alone. The folding energy of the each GAAA tetraloop module, which showed substantially negative free energy, except for '*C.* M. kahanei', is expressed in Kcal/mol in brackets.

every multiplication phase. Although point mutation must occur in both the translated and untranslated regions at the same rate, incidence of some nucleotide substitutions, observed in the prokaryotic ribozymes for housekeeping molecules, are biased by the selection of lethal mutation. These lethal mutations are not obvious in critical regions of the RNase P RNA gene. Therefore, comparison of the secondary structures may be more meaningful than the phylogenetic analysis based solely on an alignment of the RNase P RNA sequences. In conclusion, the PNS method based on the evaluation of only the strategic and highly conserved genome region in the specificity domain of RNase P RNA provides clear information at the level of heterogeneity within a species, the relatedness between species, or facilitating the characterization and clustering of specific strains.

REFERENCES

1. Birkenheuer, A.J., Breitschwerdt, E.B., Alleman, A.R. and Pitulle, C. 2002. Differentiation of *Haemobartonella canis* and *Mycoplasma haemofelis* on the basis of comparative analysis of gene sequences. *Am. J. Vet. Res.* **63**: 1385–1388.
2. Chen, Y., Carlini, D.B., baines, J.F., Parsch, J., Braverman, M., Tanda, S. and Stephan, W. 1999. RNA secondary structure and compensatory evolution. *Genes Genet. Syst.* **74**: 271–286.
3. Freier, S.M., Kierzek, R., Jaeger, J.A., Sugimoto, M., Caruthers, M.H., Nielson, T. and Turner, D.H. 1986. Improved free-energy parameters for predictions of RNA duplex stability. *Proc. Natl. Acad. Sci. U.S.A.* **83**: 9373–9377.
4. Haas, E., Banta, A.B., Harris, J.K., Pace, N.R. and Brown, J.W. 1996. Structure and evolution of ribonuclease P RNA in Gram-positive bacteria. *Nucleic Acids Res.* **24**: 4775–4782.
5. Giangaspero, M. and Harasawa, R. 2011. Species characterization in the genus *Pestivirus* according to palindromic nucleotide substitutions in the 5'-untranslated region. *J. Virol. Methods* **174**: 166–172.
6. Gultyawv, A.P., Franch, T. and Gerdes, K. 2000. Coupled nucleotide covariations reveal dynamic RNA interaction patterns. *RNA* **6**: 1483–1491.
7. Kirsebom, L.A. 2002. RNase P-mediated catalysis. *Biochem. Soc. Trans.* **30**: 1153–1158.
8. Krasilnikov, A.S., Yang, X., Pan, T. and Mondragon, A. 2003. Crystal structure of the specificity domain of ribonuclease P. *Nature* **421**: 760–764.
9. Loria, A. and Pan, T. 1996. Domain structure of the ribozyme from eubacterial ribonuclease P. *RNA* **2**: 551–563.
10. Massire, C., Jaeger, L. and Westhof, E. 1997. Phylogennetic evidence for a new tertiary interaction in bacterial RNase P RNAs. *RNA* **3**: 553–556.
11. Messsick, J.B., Walker, P.G., Raphael, W., Berent, L. and Shi, X. 2002. '*Candidatus* Mycoplasma haemodidelphidis' sp. nov., '*Candidatus* Mycoplasma haemolamae' sp. nov. and *Mycoplasma* haemocanis comb. nov., haemotrophic parasites from a naturally infected opossum (*Didelphis virginianna*), alpaca (*Lama pacos*) and dog (*Canis familiaris*): phylogenetic and secondary structural relatedness of their 16S rRNA genes to other mycoplasmas. *Int. J. Syst. Evol. Microbiol.* **52**: 693–698.
12. Peters, I.R., Helps, C.R., McAuliffe, L., Neimark, H., Lappin, M.R., Gruffydd-Jones, T.J., Day, M.J., Hoelzle, L. E., Willi, B., Meli, M., Hofmann-Lehmann, R. and Tasker, S. 2008. RNase P RNA gene (*rnpB*) phylogeny of hemoplasmas and other *Mycoplasma* species. *J. Clin. Microbiol.* **46**: 1873–1877.
13. Siegel, R.W., Banta, A.B., Haas, E.S., Brown, J.W. and Pace